LA-UR- 11-04812

Approved for public release; distribution is unlimited.

Title:	An Overview of High-Pressure Synchrotron Researches
Author(s):	Yusheng Zhao
Intended for:	Xian-Shan meeting on extreme experimental conditions, Beijing, Aug 29-Sept 1, 2011 Invited presentation

Los Alamos
NATIONAL LABORATORY
EST. 1943

Form 836 (7/06)




An Overview of High-Pressure Synchrotron Researches

Yusheng Zhao

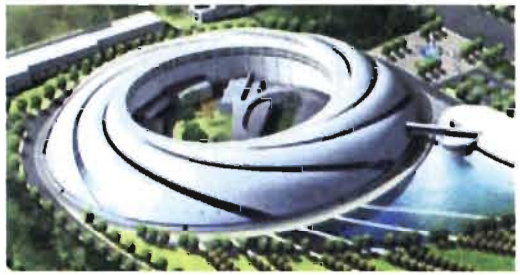

LANSCE – Lujan Center
Los Alamos National Laboratory

HiPSEC (a DOE/NNSA Center of Excellence)
University of Nevada Las Vegas

High Pressure Research using SR

All top notch SR light sources dedicate beamlines *for high pressure studies*

APS – GSECARS and HPCAT

Diamond Anvil Cell and Large Volume Multi-Anvil PRESS

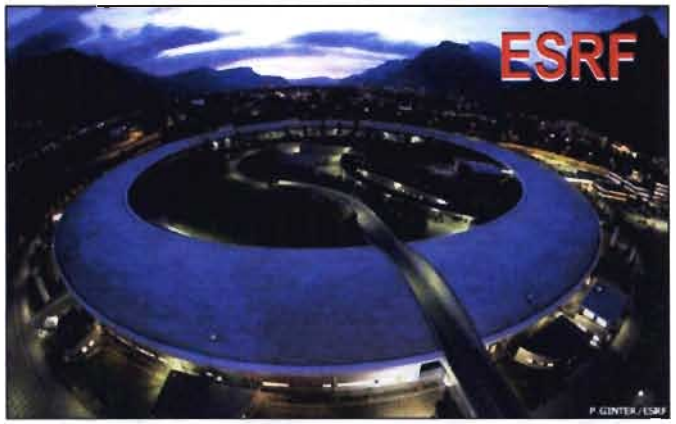

ESRF – ID16, BM29, ID27 and ID06

SPring8 - BL04B1, BL14B1 and BL22XU

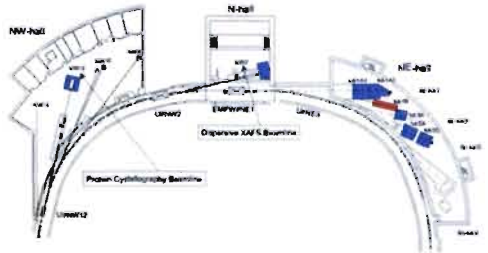

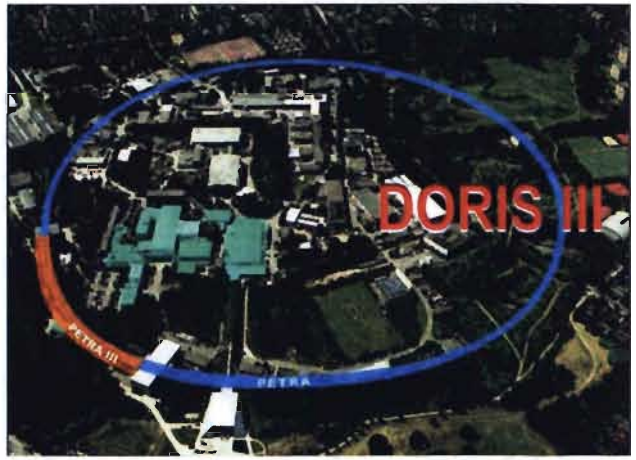

NSLS-X17; PF-AR NE5C; DORISIII-F2.1

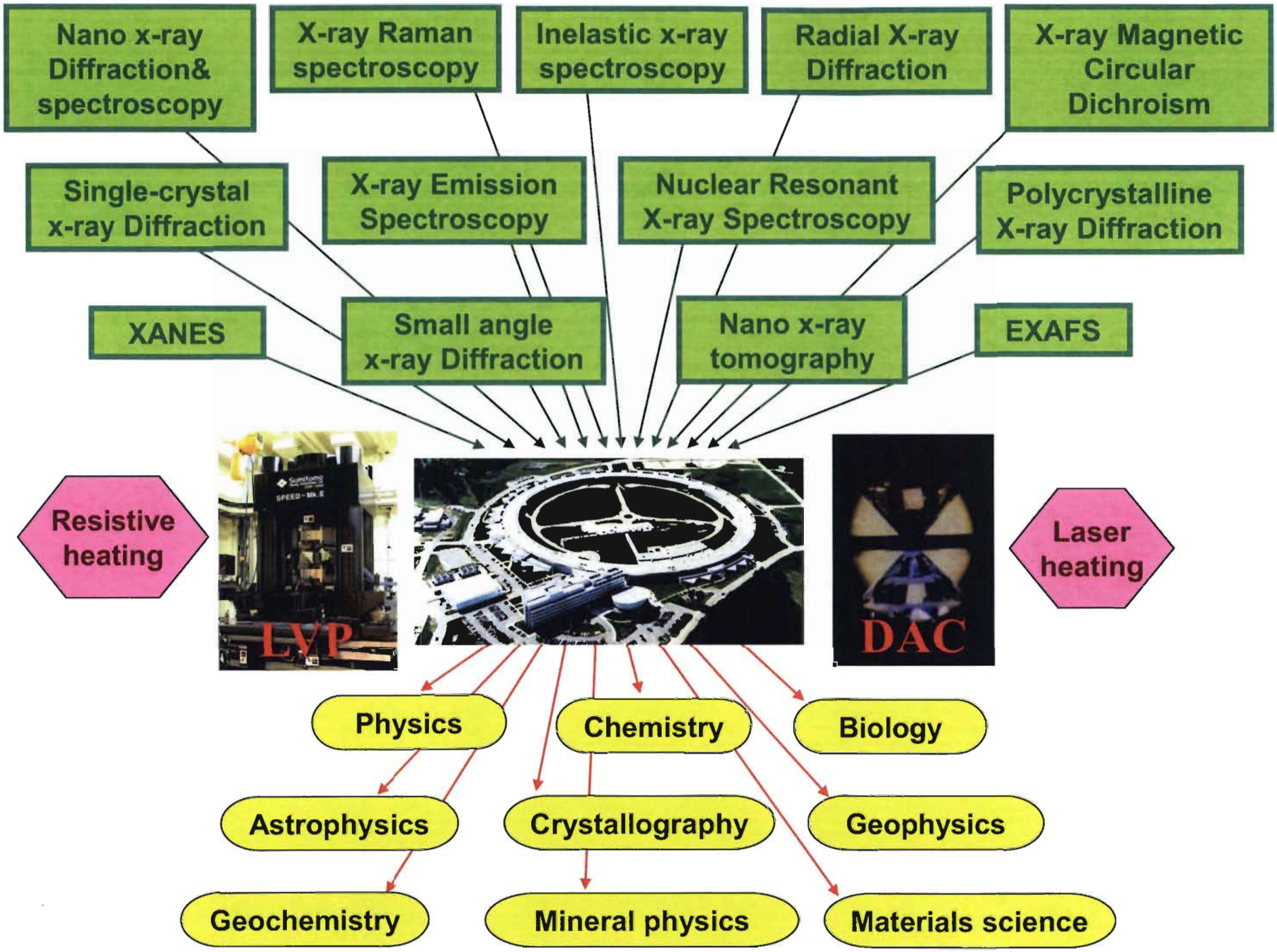
Nano x-ray Diffraction& spectroscopy
X-ray Raman spectroscopy
Inelastic x-ray spectroscopy
Radial X-ray Diffraction
X-ray Magnetic Circular Dichroism
Single-crystal x-ray Diffraction
X-ray Emission Spectroscopy
Nuclear Resonant X-ray Spectroscopy
Polycrystalline X-ray Diffraction
XANES
Small angle x-ray Diffraction
Nano x-ray tomography
EXAFS
Resistive heating
LVP
DAC
Laser heating
Physics
Chemistry
Biology
Astrophysics
Crystallography
Geophysics
Geochemistry
Mineral physics
Materials science

Minerals

Earth Sciences

Materials

Advanced Ceramics/Alloys

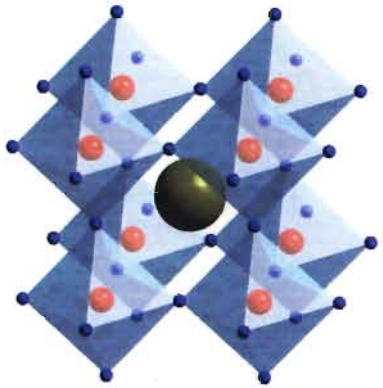

Crystal Structure Refinement

P-T-V Equation of State

P-T-X Phase Diagram

Constitutive Properties

nano-Science/Technology

X-Ray Radiography/Tomography

Acoustic Elasticity & Thermo-Calorimetry

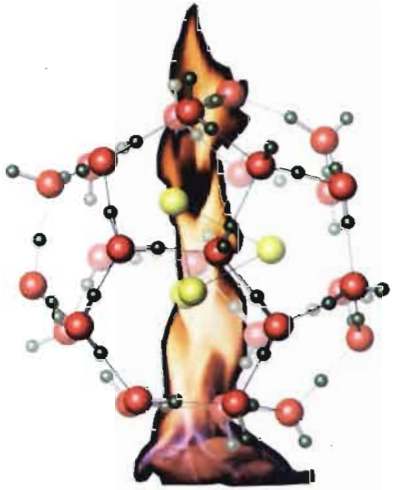

Instrumentation Developments

Energy Material Explorations

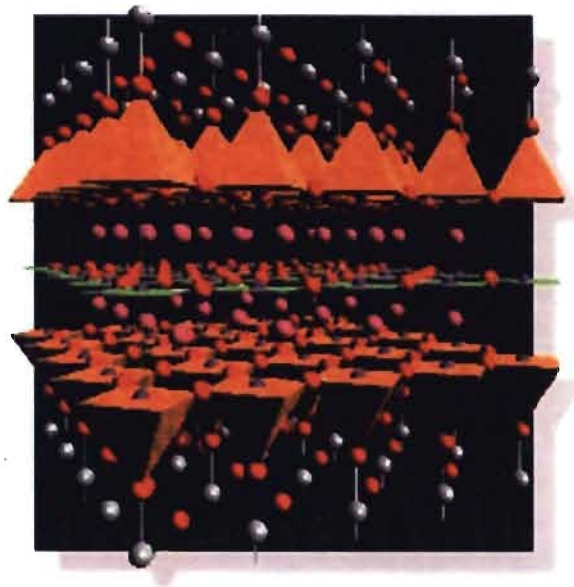

Crystal structure of high-T_c superconductor was first successfully determine by neutron diffraction (the classic '1-2-3' YBa2Cu3O7-x superconductor, published on *Nature* on 28 May 1987).

The neutron also first determined the antiferromagnetic interaction strength between copper electrons in the parent high-T_c La2CuO4.

Neutron study of HgBa2CuO4+d has revealed the structural basis for strong dependence of superconducting T_c on applied pressure.

Searching superconductors in P-T-X space

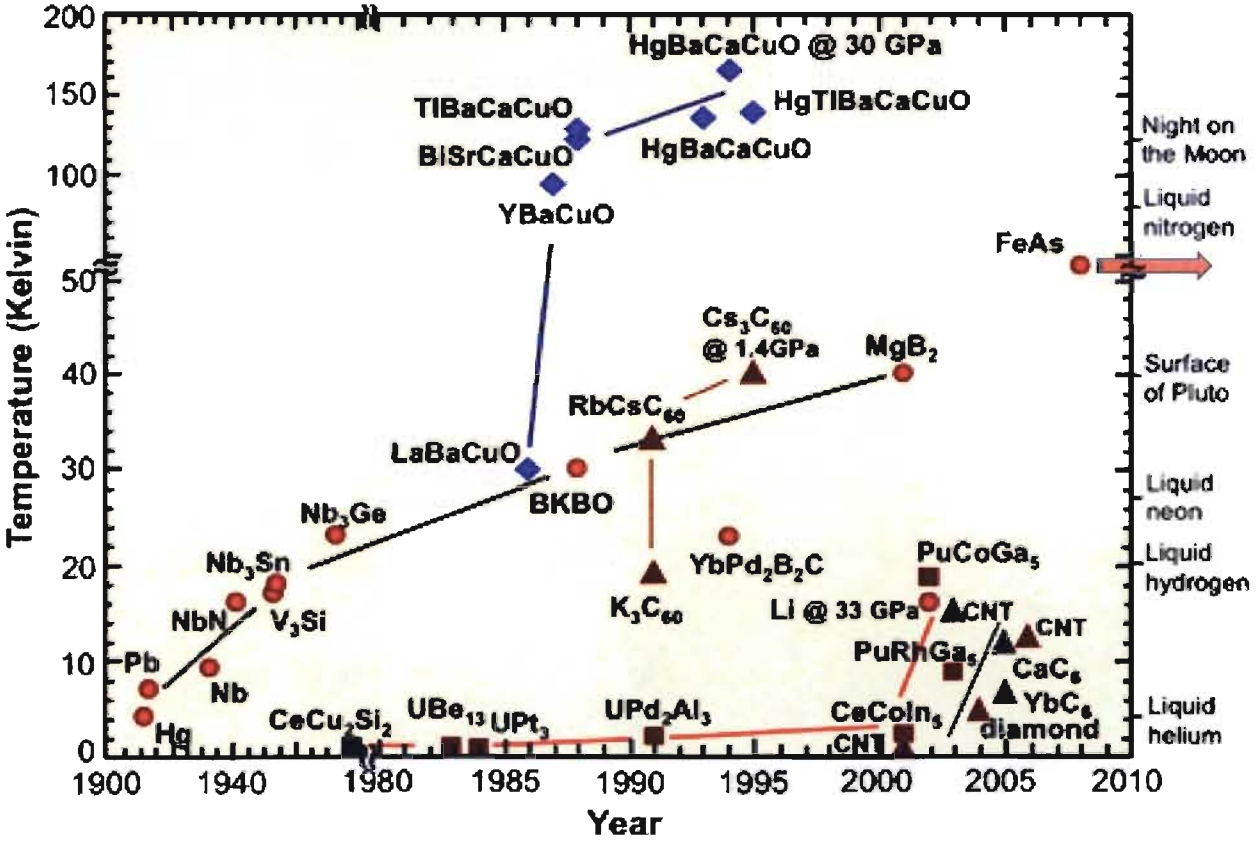

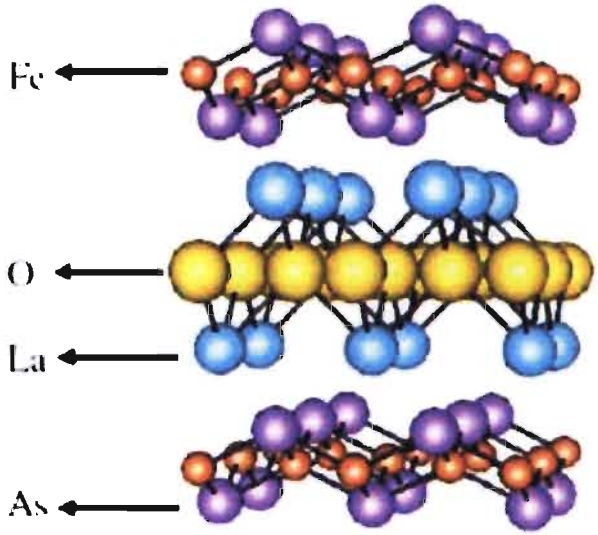

1111

Tetragonal

P4/nmm

Sm based iron SC 53 K

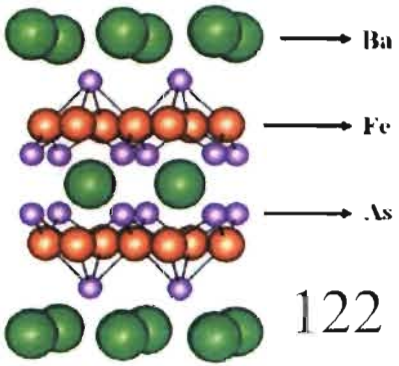

Tetragonal
I4/mmm

Aswathy *et al.*,
Supercond.Sci.Tech.
23, 073001 (2010)

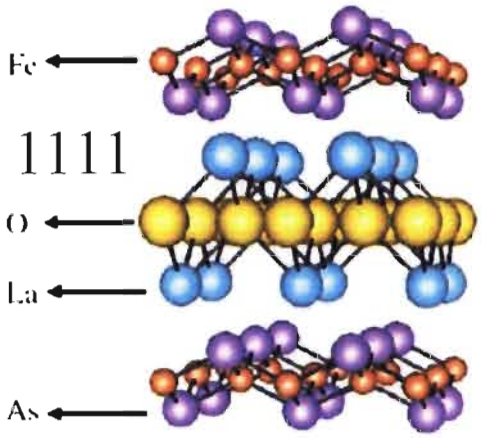

Tetragonal
P4/nmm

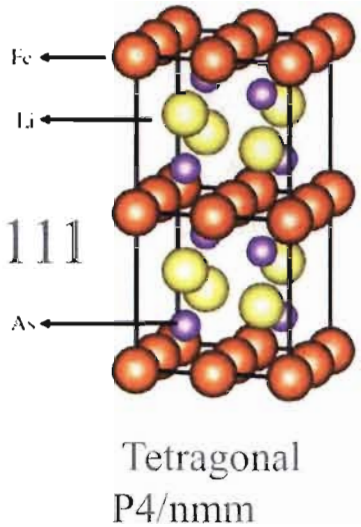

Tetragonal
P4/nmm

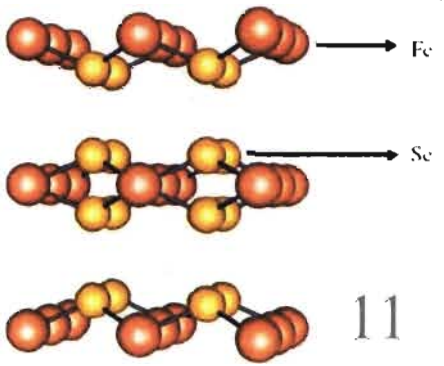

Tetragonal
P4/nmm

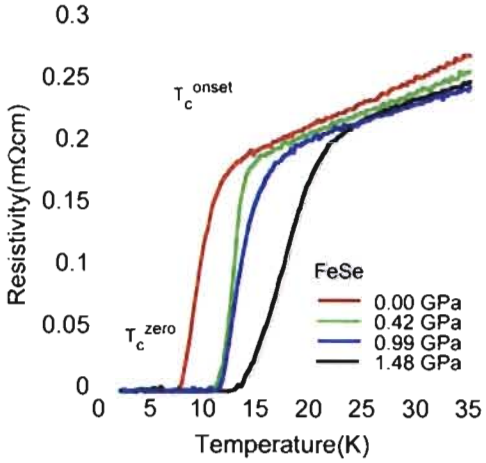

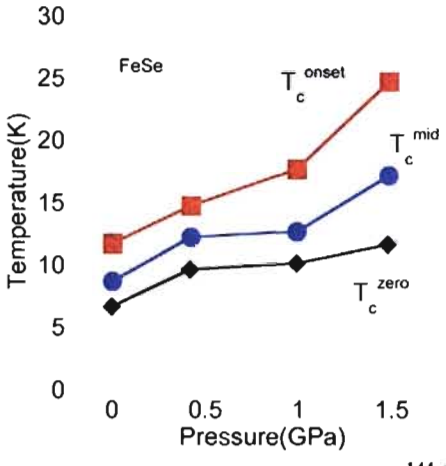

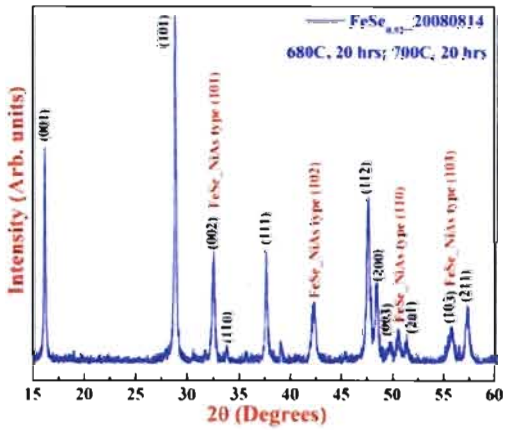

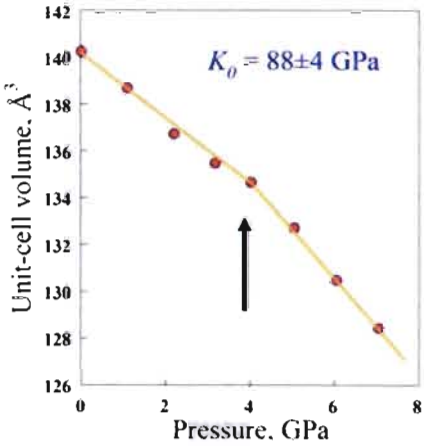

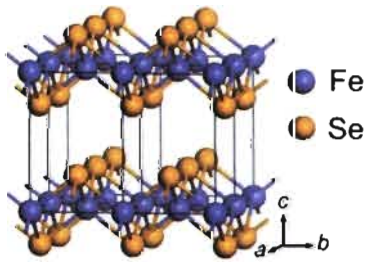

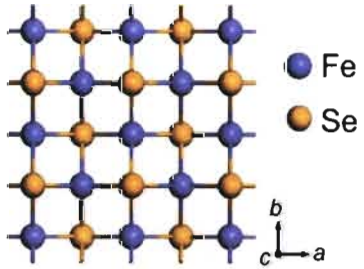

Figure 1 | Schematic crystal structure of *α*-FeSe. Four unit cells are shown to

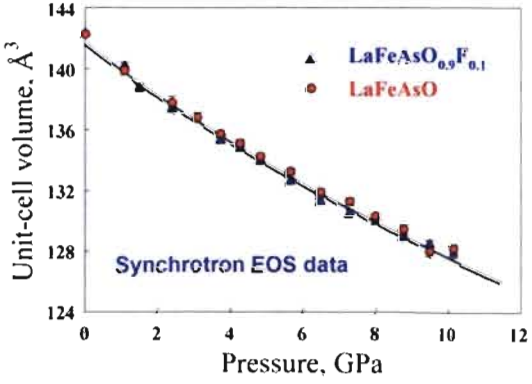

Neutron diffraction EOS data for $LaO_{0.9}F_{0.1}FeAs$
Note that there is a kink at about 4 GPa

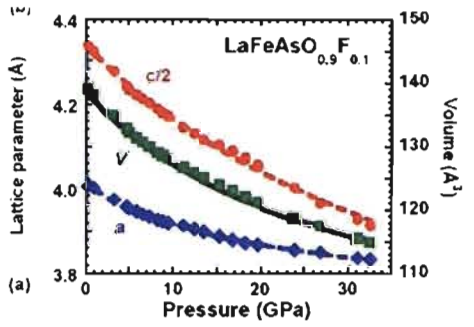

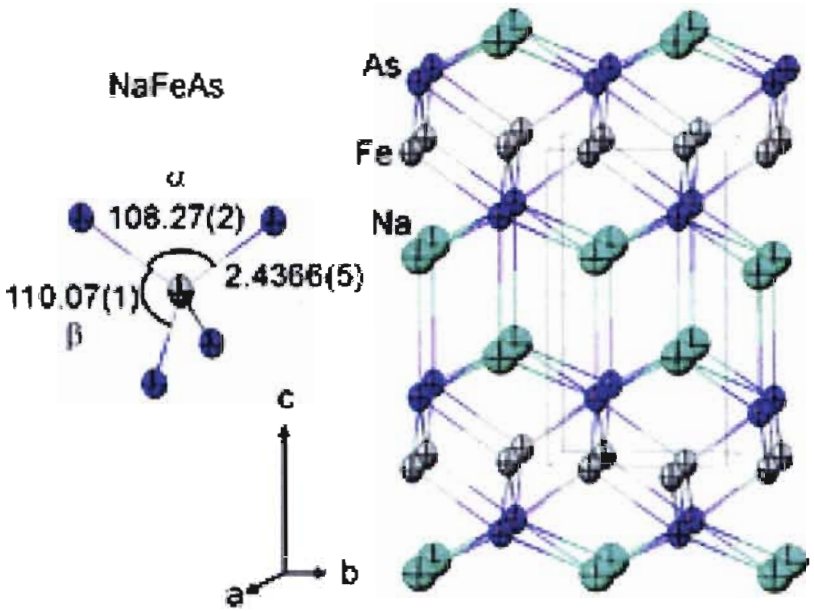
NaFeAs
α
108.27(2)
110.07(1)
2.4366(5)
β
As
Fe
Na
c
b
a

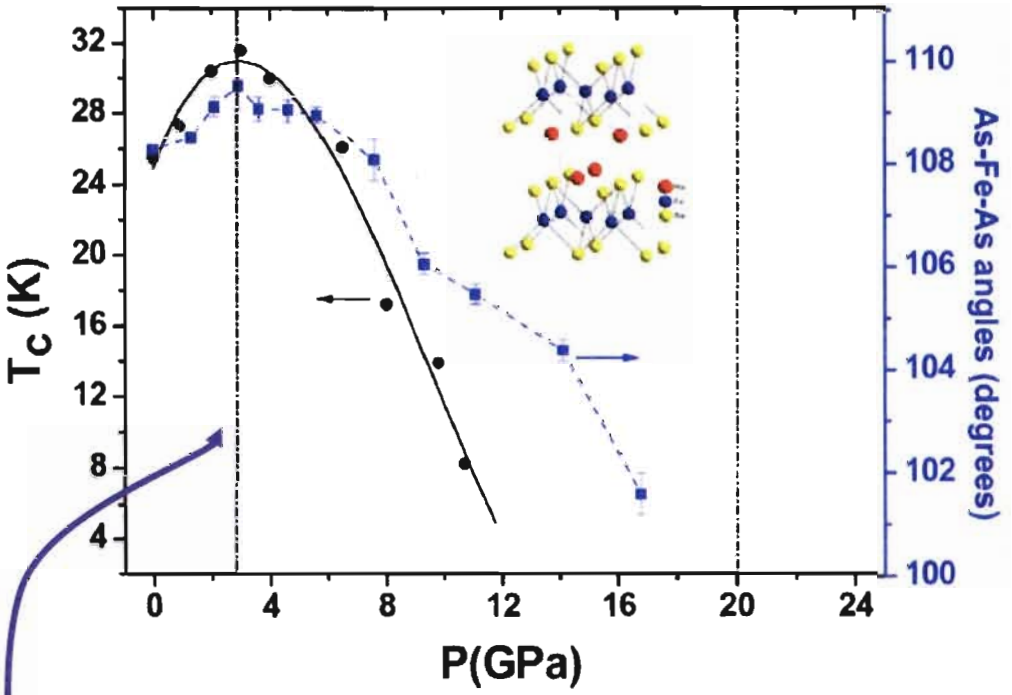
T_c (K)
As-Fe-As angles (degrees)
P(GPa)

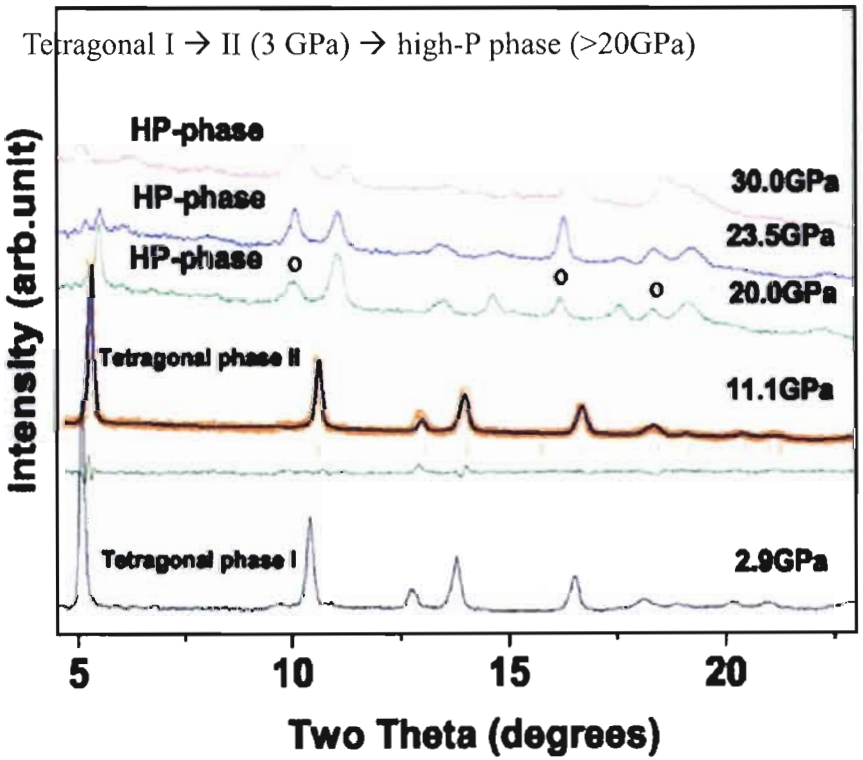
Tetragonal I → II (3 GPa) → high-P phase (>20GPa)
HP-phase
HP-phase
HP-phase
30.0GPa
23.5GPa
20.0GPa
Tetragonal phase II
11.1GPa
Tetragonal phase I
2.9GPa
Intensity (arb.unit)
Two Theta (degrees)

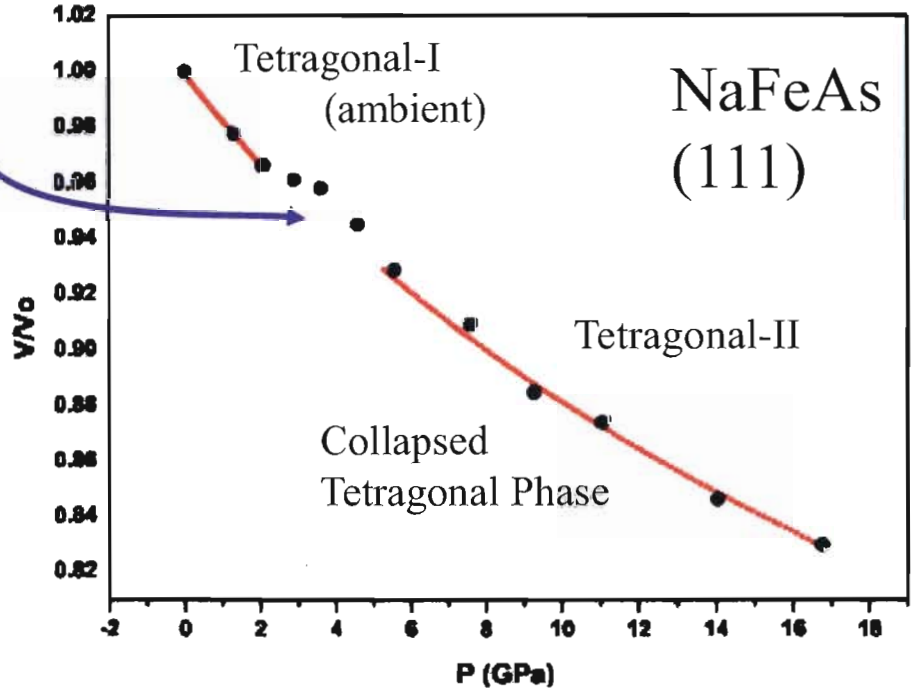
Tetragonal-I
(ambient)
NaFeAs
(111)
Tetragonal-II
Collapsed
Tetragonal Phase
V/Vo
P (GPa)

Initial enhancement of bulk modulus observed for the nano-ceramics may result from the "pre-" **compressed** surface lattices in the **shell** volume of the nano- crystal grains;

The high pressure induced work-weakening/cold-welding type of grain growth ***fuse*** surface shell with bulk cores, correspondingly the elastic modulus reduces/approaches the bulk values at high-pressures after P_c.

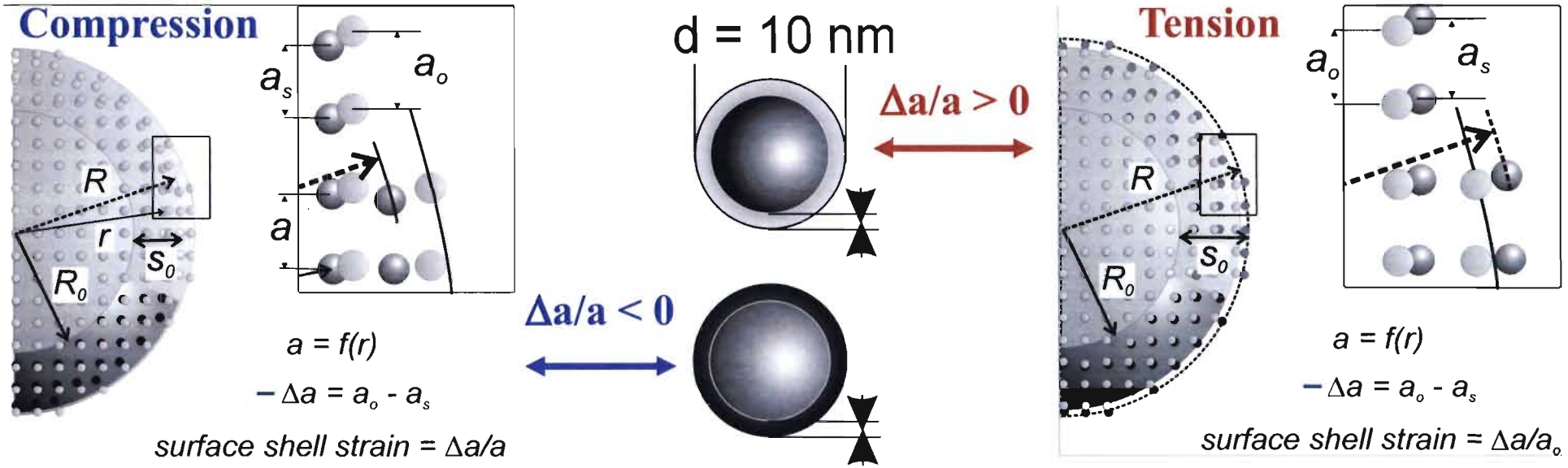

Initial reduction of bulk modulus observed for the nano-metals may result from "pre-" **expanded** surface lattices in the **shell** volume of the nano- crystal grains;

High pressure induced work-hardening after the bulk yield reflects continuous densification of the surface shell while bulk core also experience compression.

(a), relaxed lattice

(no stress applied on the "infinite" atomic lattices)

(b), macro-strains

(stress field applied to the overall sample)

(c), micro-strains

(stress concentration due to grain-to-grain contacts)

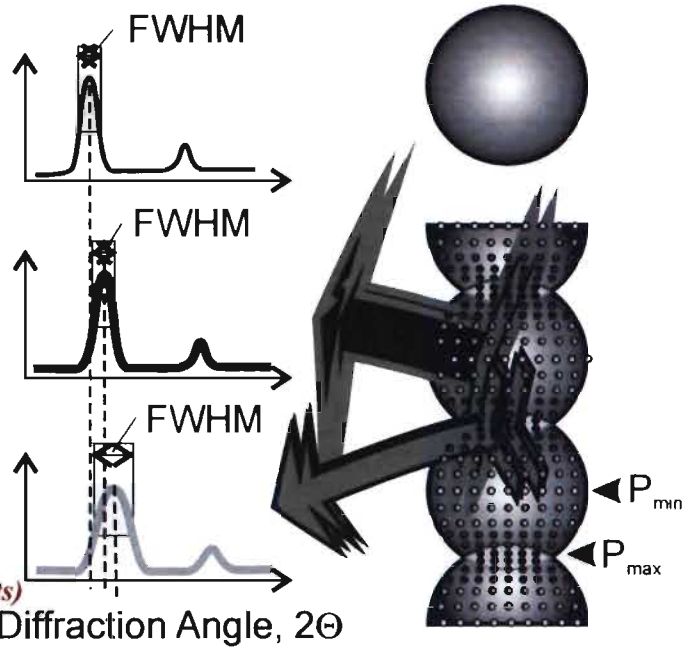

The strain imposed by applied stresses & by *grain-to-grain* stress concentration at contact points

nano-crystal **Uniform Core and Strained Surface** ***Palosz* Model**

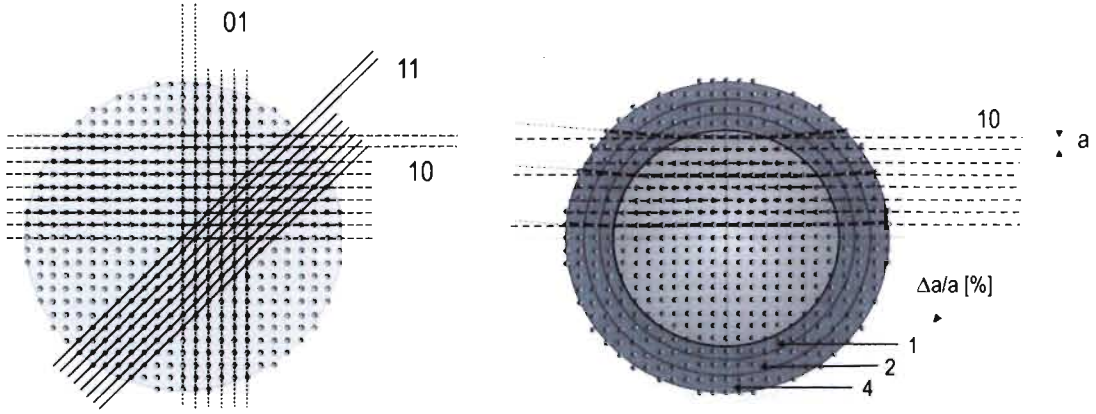

(a) (b)

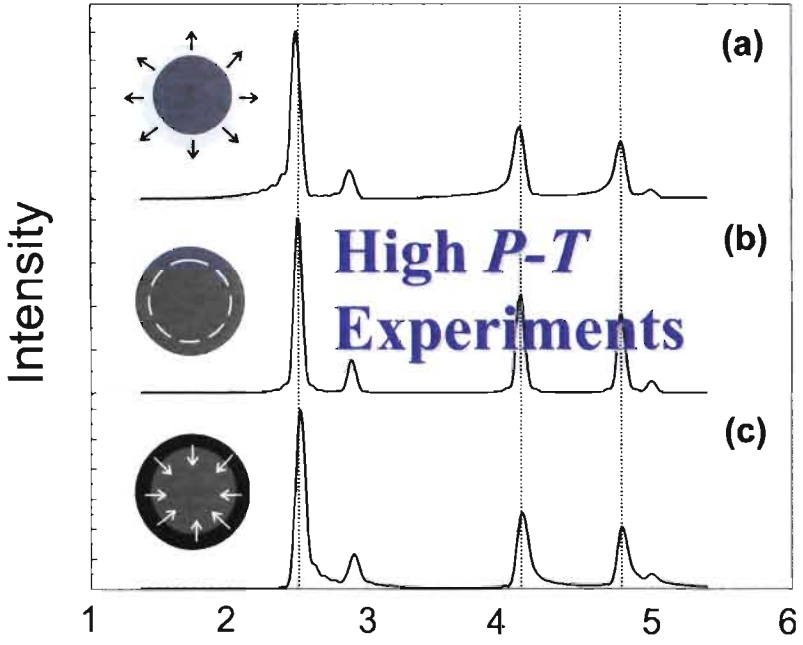

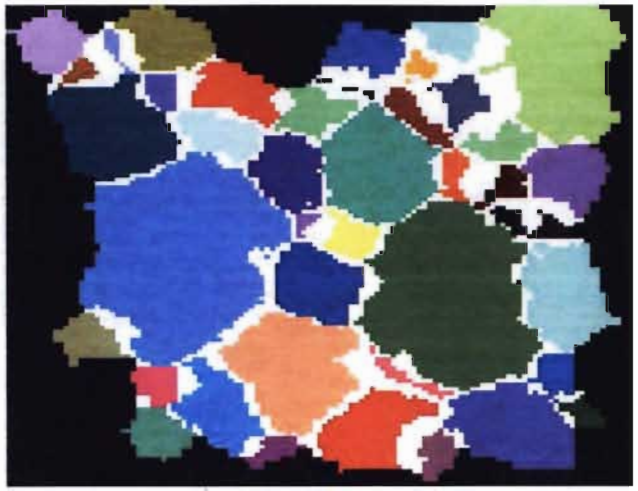

Macro- *vs* micro-

under pressures

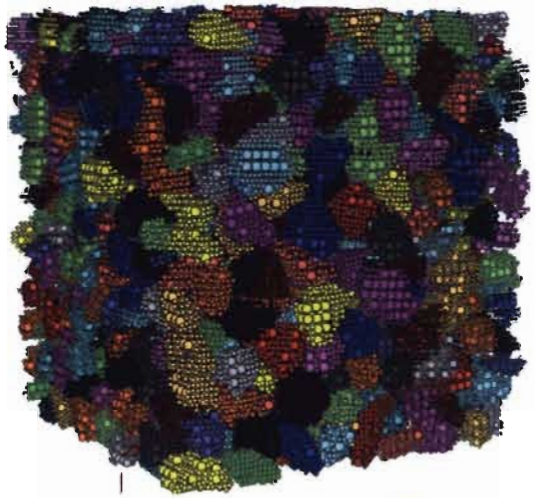

Powder Compaction

(micro-strain)

Deviatoric Stress

(macro-strain)

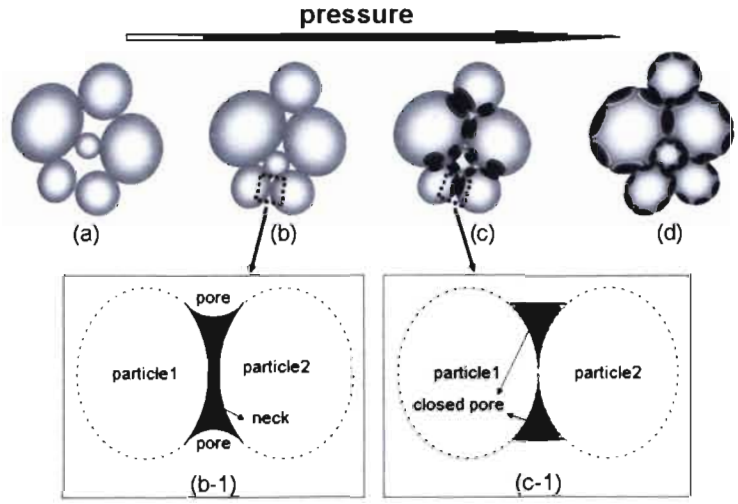

***grain-to-grain* contact stress concentration**

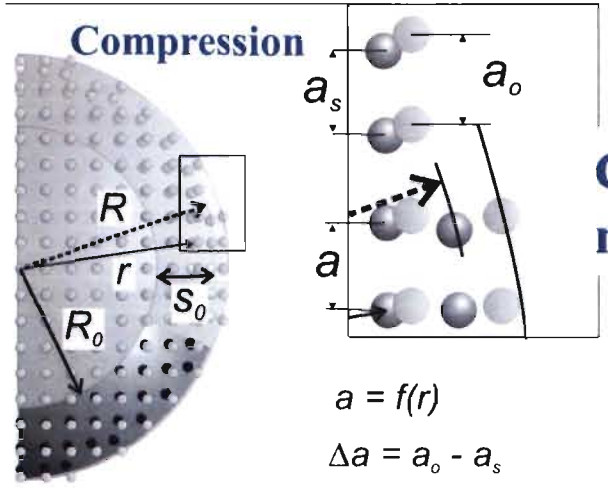

Ceramic nano-TiO_2

$a = f(r)$

$\Delta a = a_o - a_s$

$a_s < a_o$

surface shell strain = $\Delta a/a$

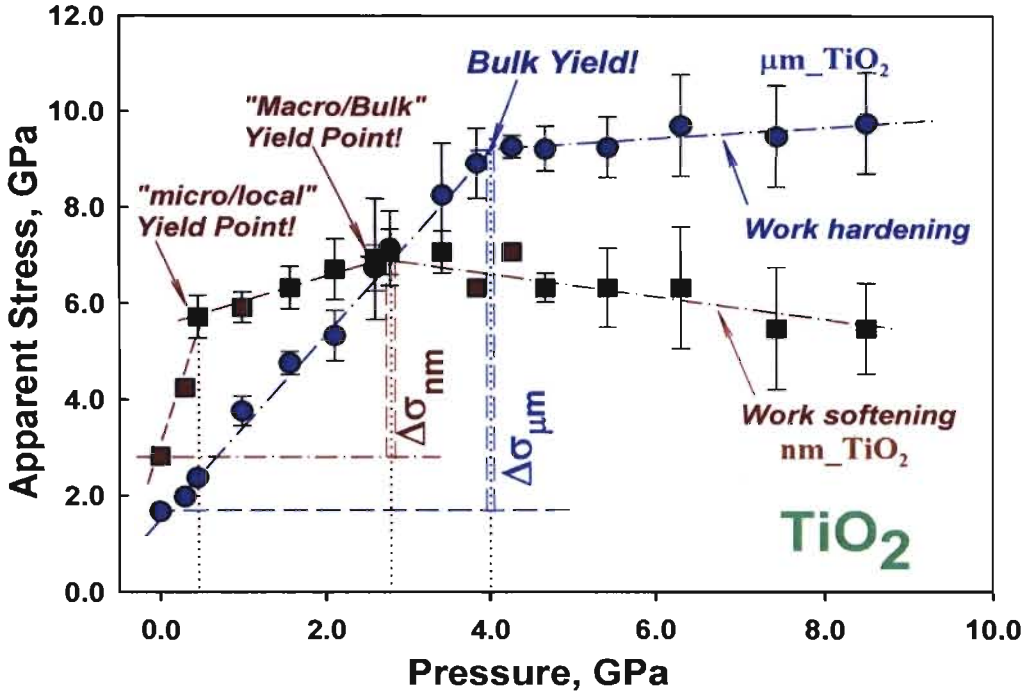

Ceramic nano-TiO_2 with compressed shell shows work-weakening under stress (P)

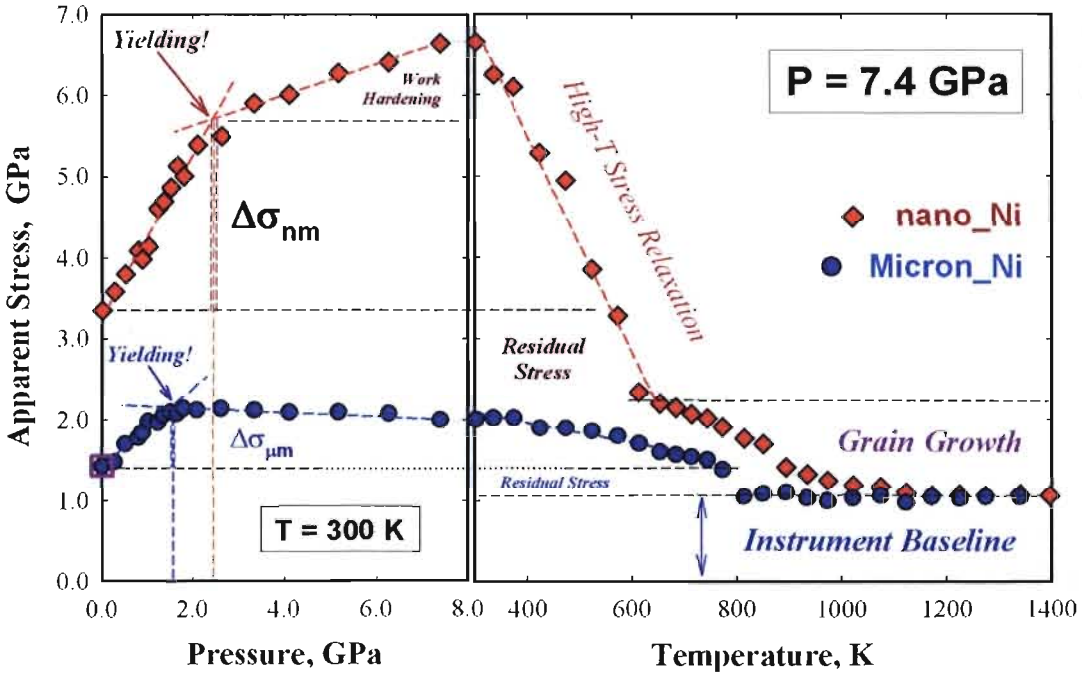

Metal nano-Ni with tensile shell shows work-hardening under stress (P)

Metal nano-Ni

$a_s > a_o$

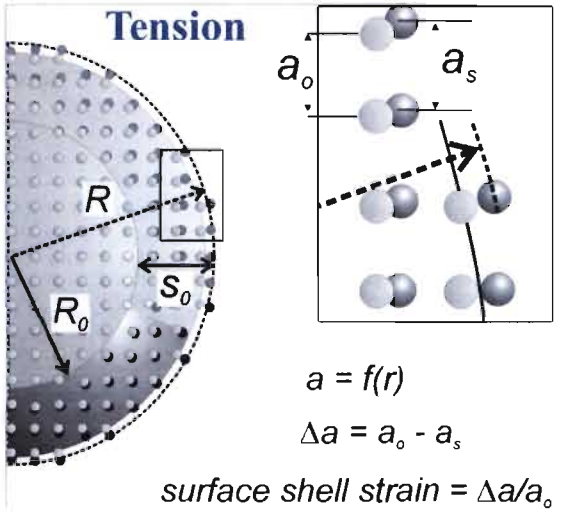

$a = f(r)$

$\Delta a = a_o - a_s$

surface shell strain = $\Delta a/a_o$

Characterization of the B-C-N sample

Vickers hardness measurement of BC_2N

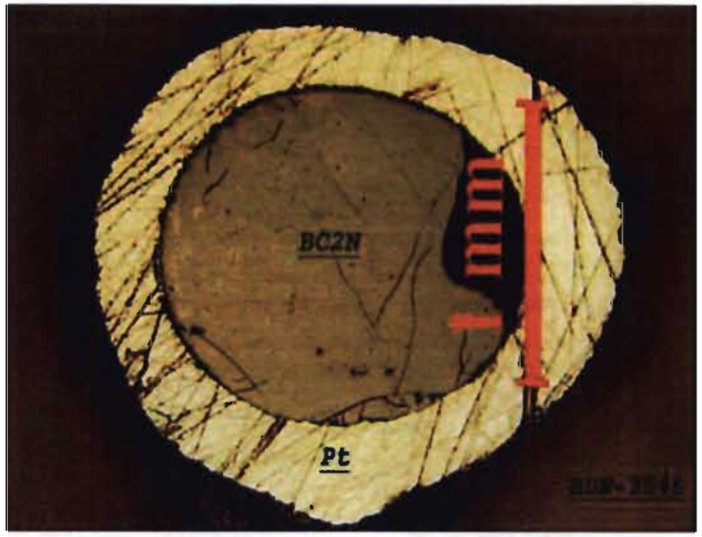

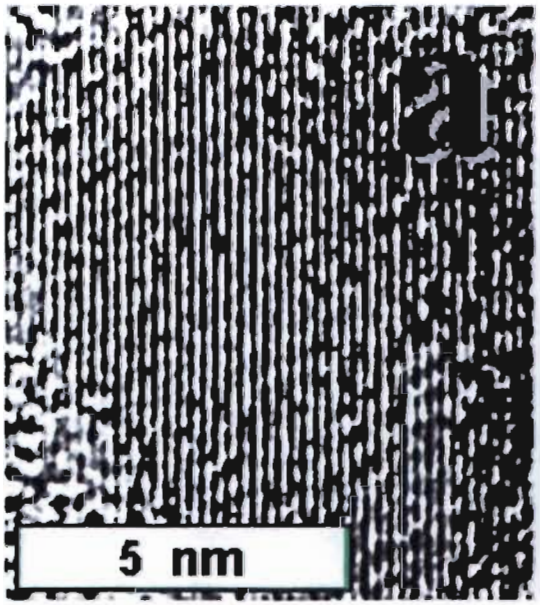

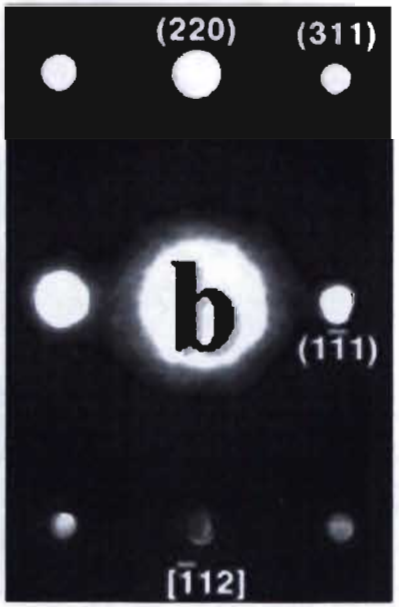

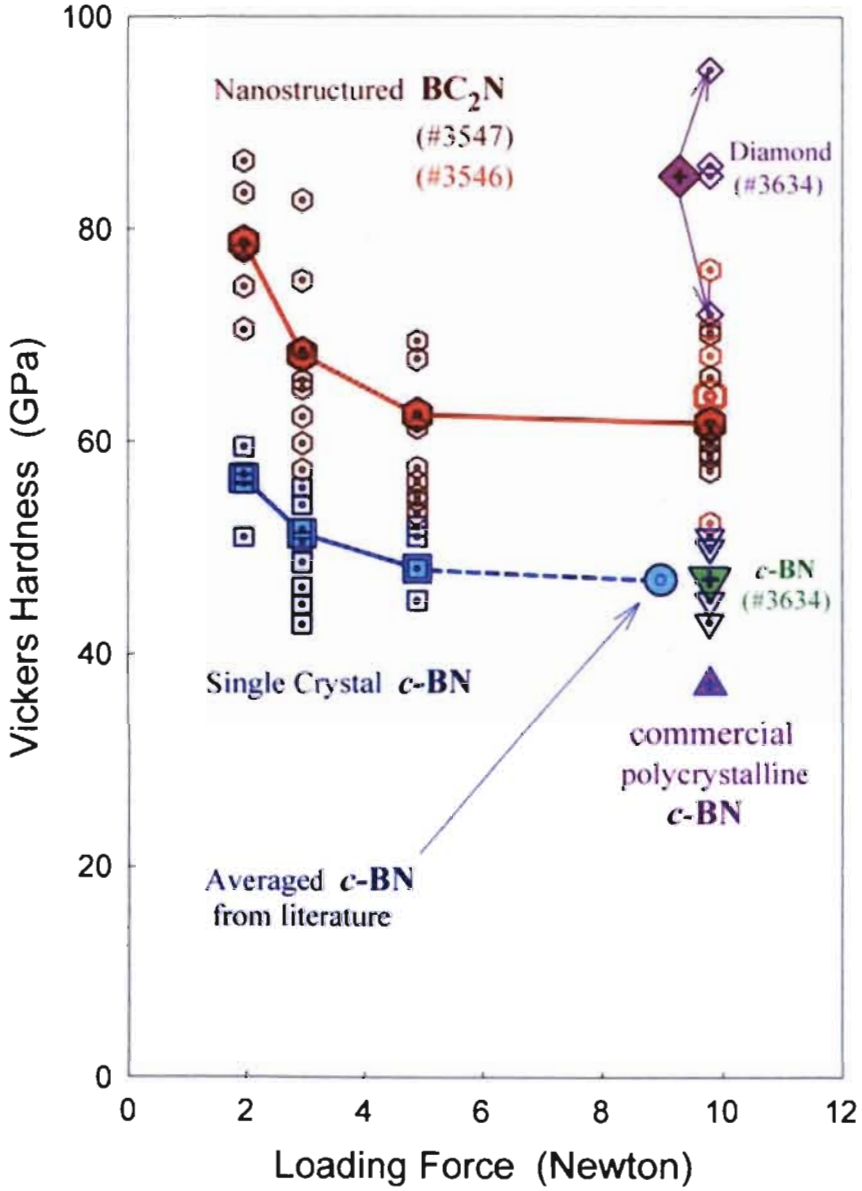

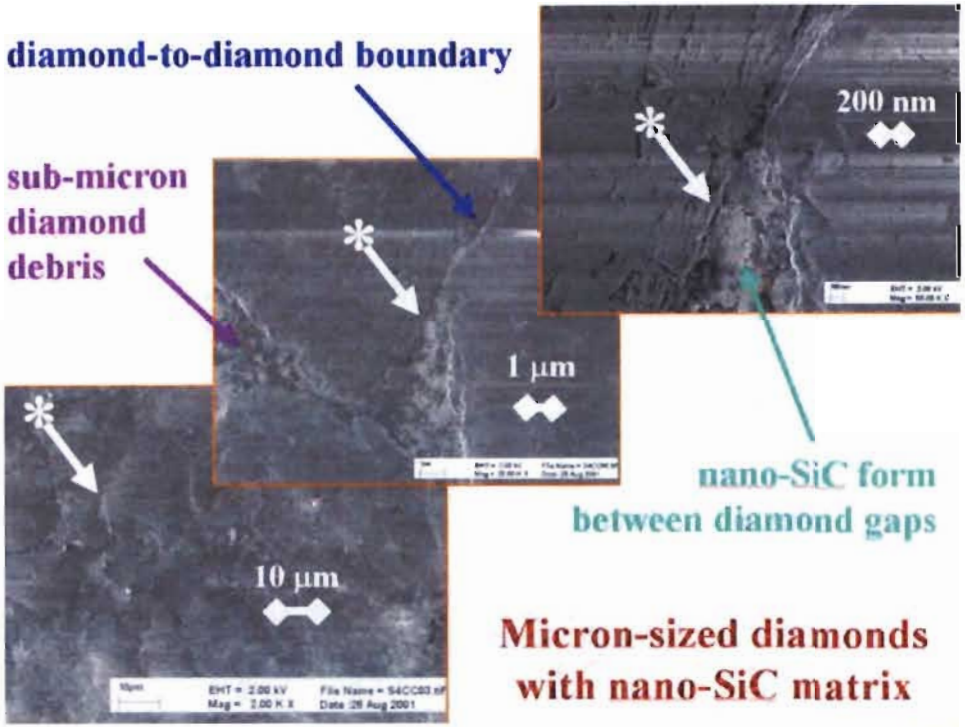
diamond-to-diamond boundary
sub-micron diamond debris
200 nm
1 μm
10 μm
nano-SiC form between diamond gaps
Micron-sized diamonds with nano-SiC matrix

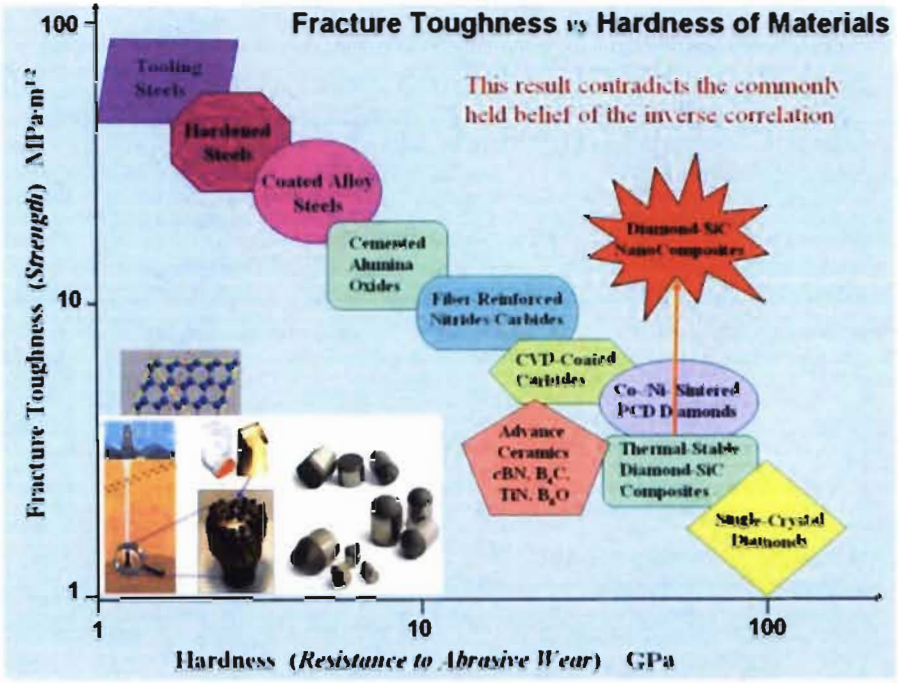
Fracture Toughness vs Hardness of Materials
This result contradicts the commonly held belief of the inverse correlation
Tooling Steels
Hardened Steels
Coated Alloy Steels
Cemented Alumina Oxides
Fiber Reinforced Nitrides Carbides
CVD-Coated Carbides
Advance Ceramics cBN, B4C, TiN, B6O
Diamond-SiC NanoComposites
Co-Ni Sintered PCD Diamonds
Thermal-Stable Diamond-SiC Composites
Single-Crystal Diamonds
Fracture Toughness (Strength) MPa·m1/2
Hardness (Resistance to Abrasive Wear) GPa
100
10
1
1
10
100

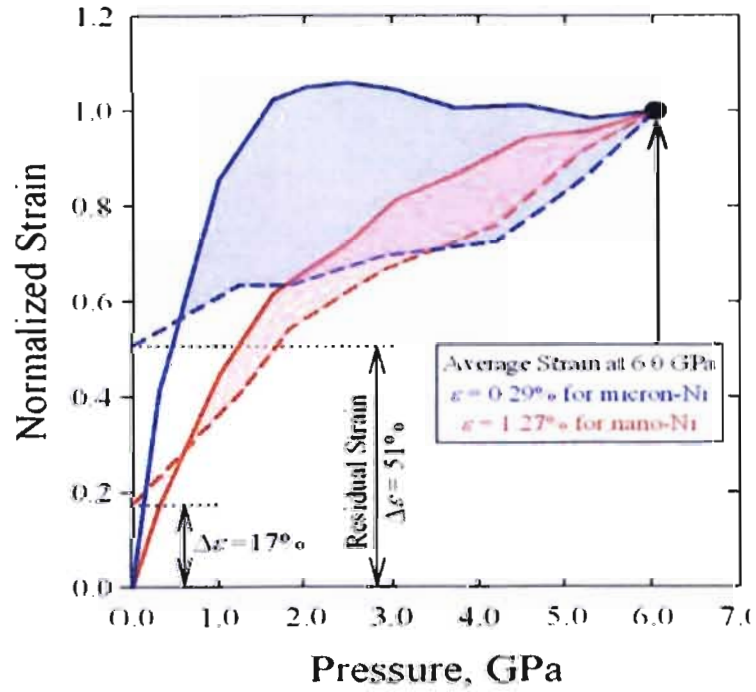
Normalized Strain
Pressure, GPa
Average Strain at 6.0 GPa
ε = 0.29% for micron-Ni
ε = 1.27% for nano-Ni
Residual Strain
Δε = 51%
Δε = 17%

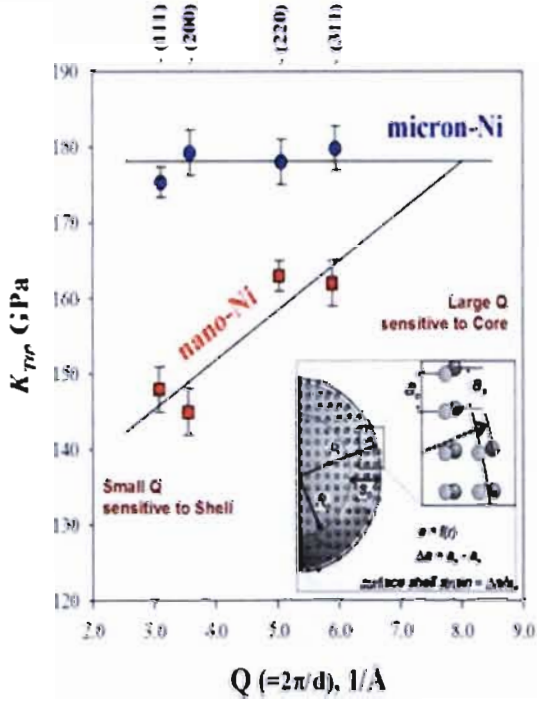
micron-Ni
nano-Ni
Large Q sensitive to Core
Small Q sensitive to Shell
Q (=2π/d), 1/Å

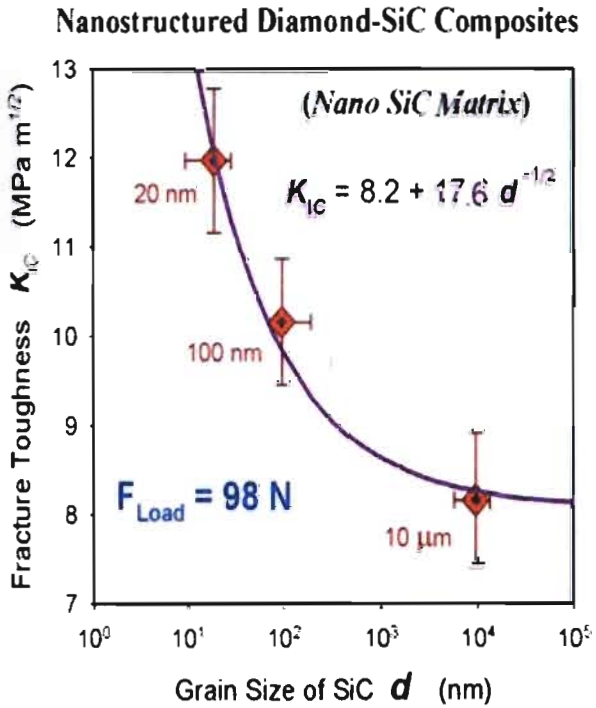
Nanostructured Diamond-SiC Composites
(Nano SiC Matrix)
K_{IC} = 8.2 + 17.6 $d^{-1/2}$
20 nm
100 nm
10 μm
F_{Load} = 98 N
Fracture Toughness K_{IC} (MPa m$^{1/2}$)
Grain Size of SiC d (nm)

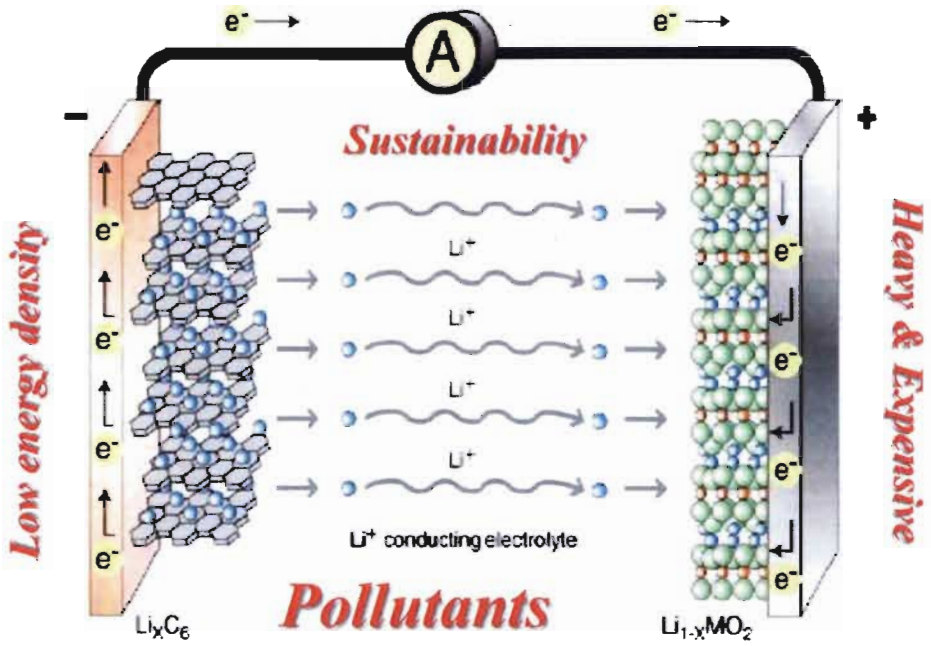

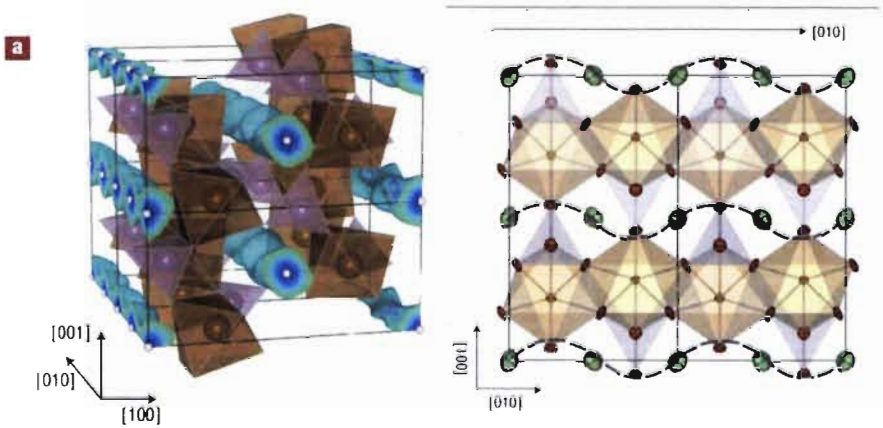

The molecular encapsulation and pressurizing effects has inspired us to investigate high lithium storage possibility. Conducting MOFs, zeolites, and clathrates offer a route to design the nano-architecture of electrode with high specific energy (high Li density!) .

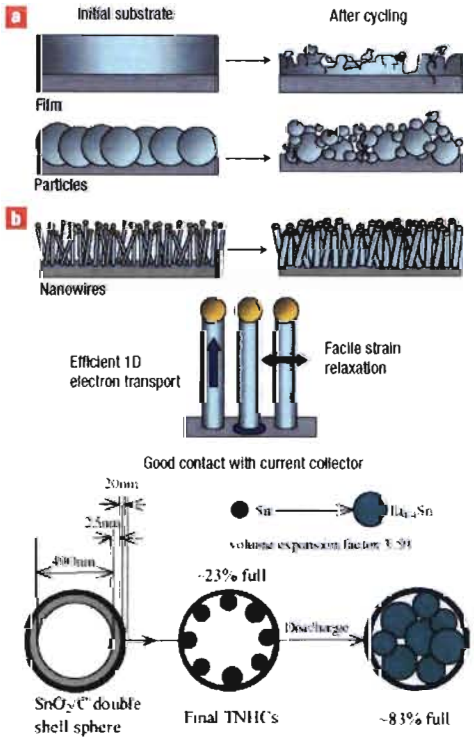

Problems!!!

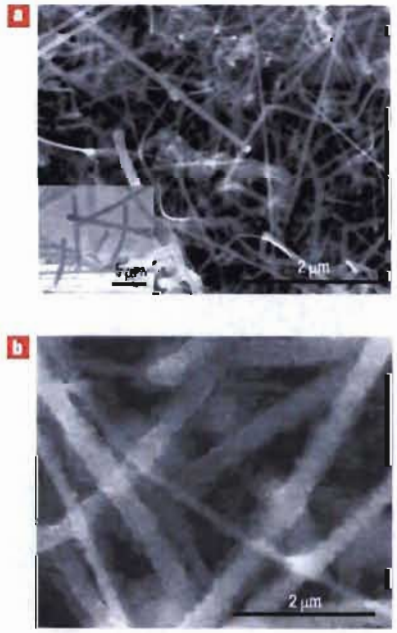

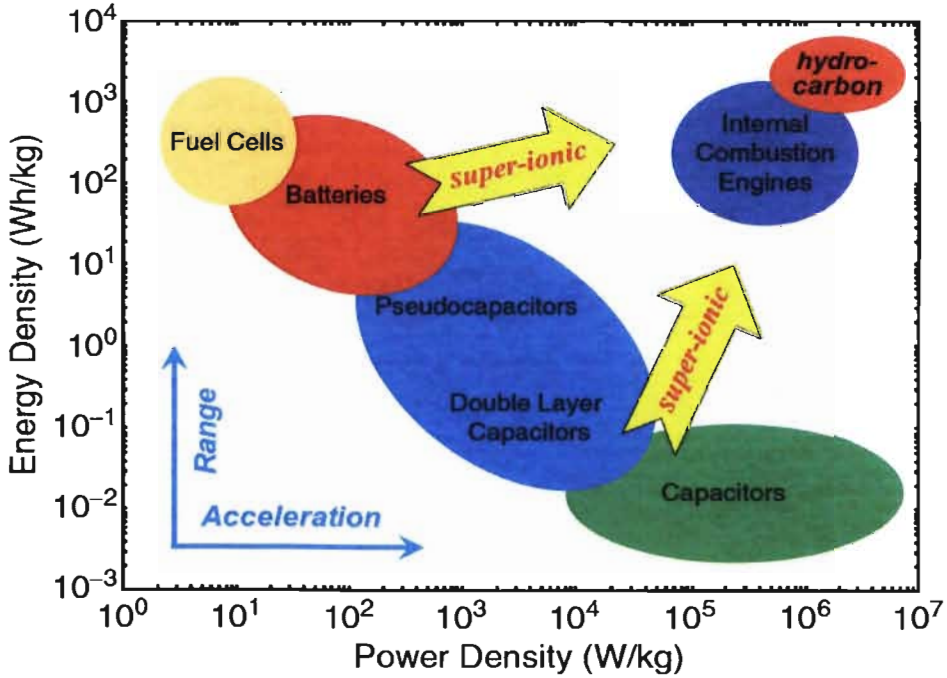

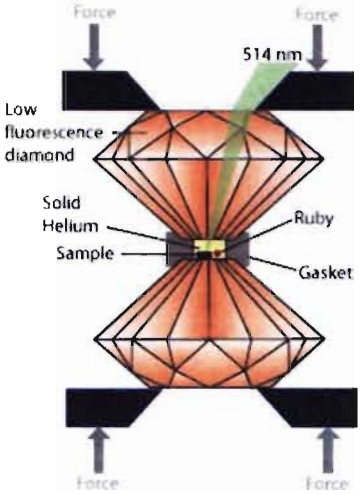

Diamond Anvil Cell

Multi-Anvil

Toroidal Anvil

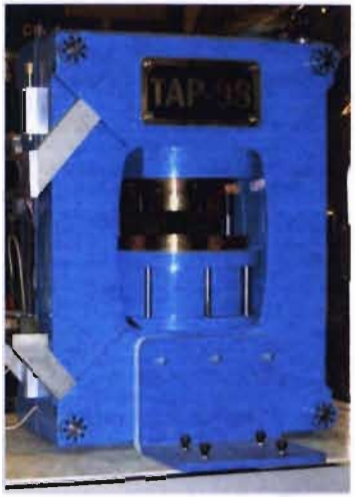

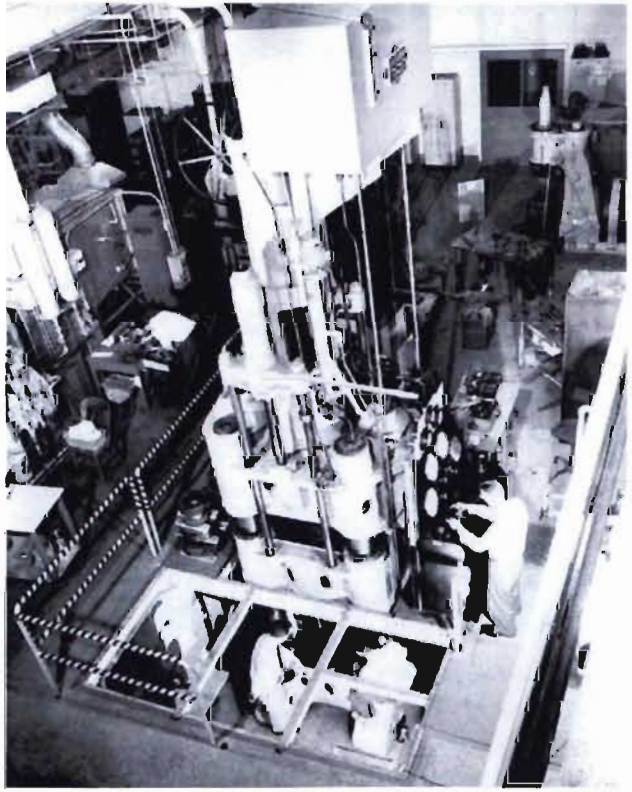

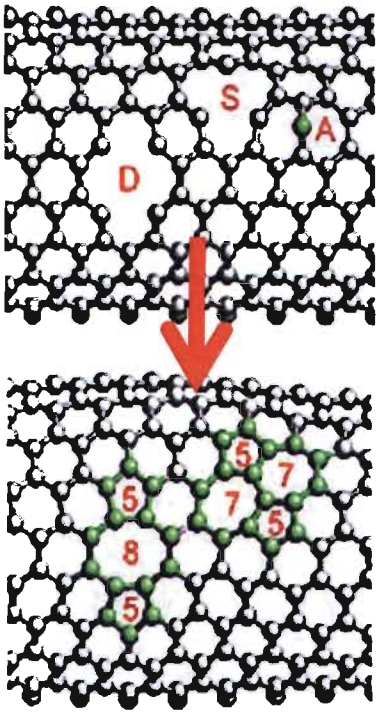

High-Pressure Microscopy
nanotube as a high-P squeezer!

Diamond anvil cell

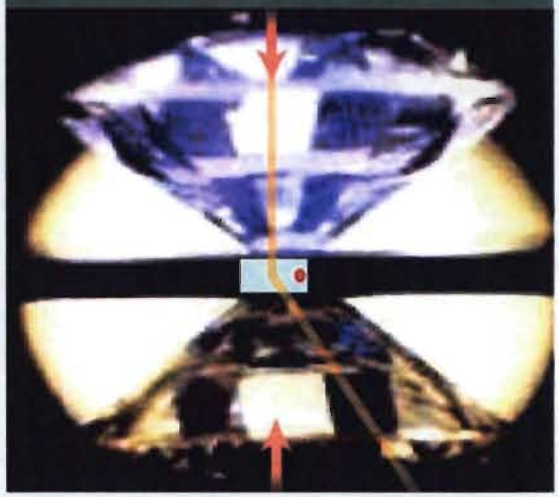

Carbon nanotube cell

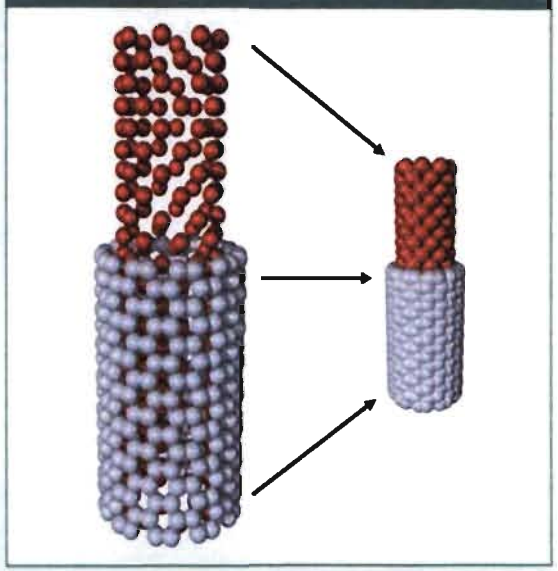

In situ x-ray diffraction

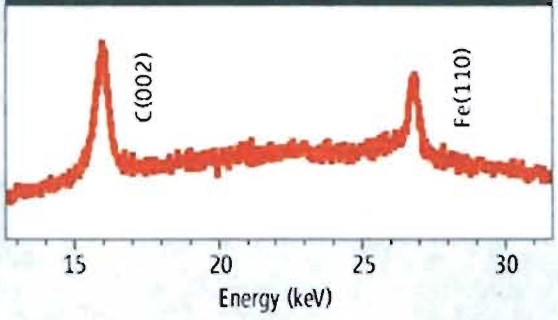

In situ electron microscopy

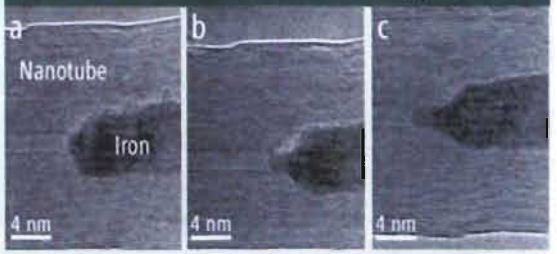

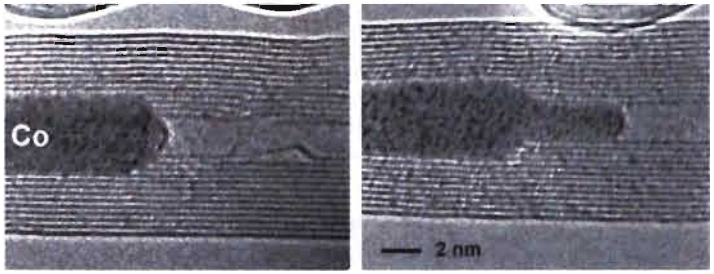

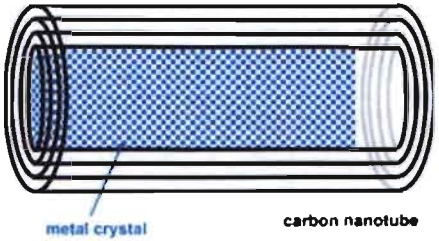

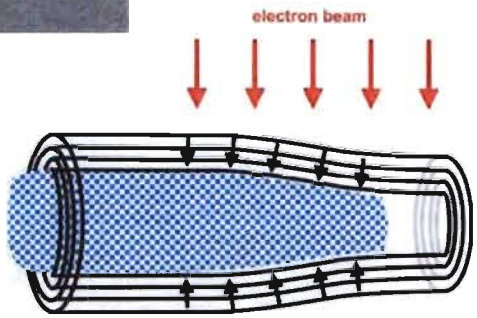

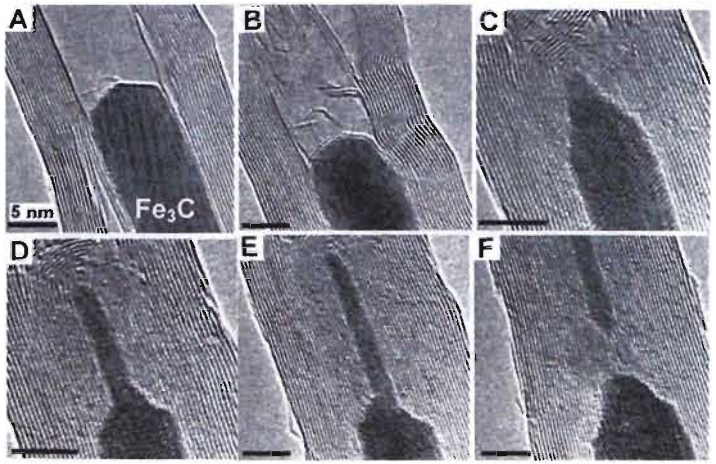

host-guest interactions (quantum clustering)

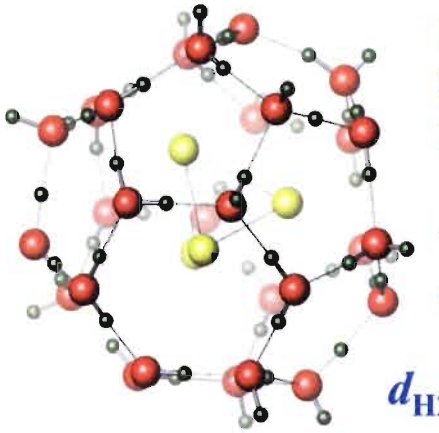

Hydrogen Clathrate Hydrate

Cage Structure

$d_{H2\text{-}H2} \sim 2.9$ Å

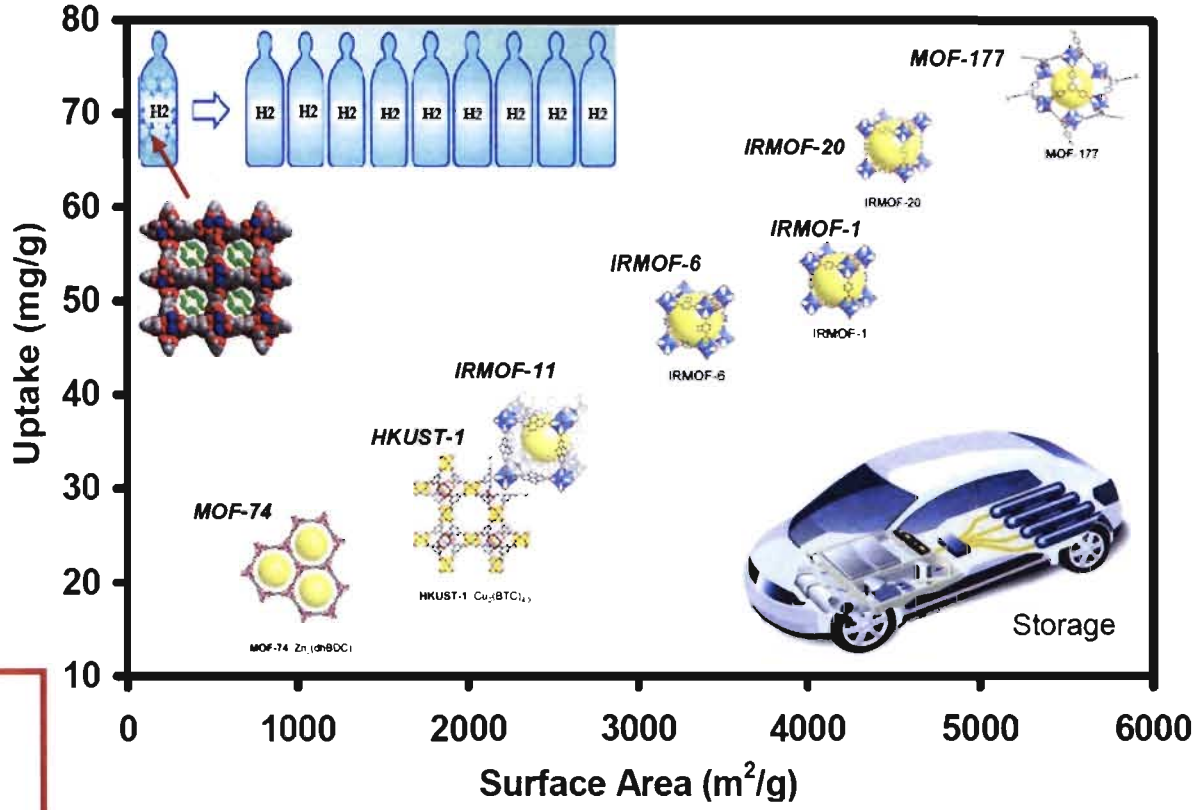

20~22% reduction of the bond length in *hydrogen cluster* need to apply as much as 10's kbar in pressure !!!

$d_{H2\text{-}H2} \sim 3.76$ Å

$d_{H2\text{-}H2} \sim 3.0$ Å

The host nano-encapsulation shows strong ***pressurizing*** effects applied on the guest

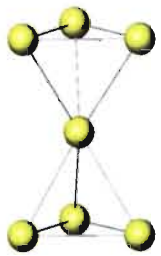

Solid Hydrogen

Metal-Organic Framework

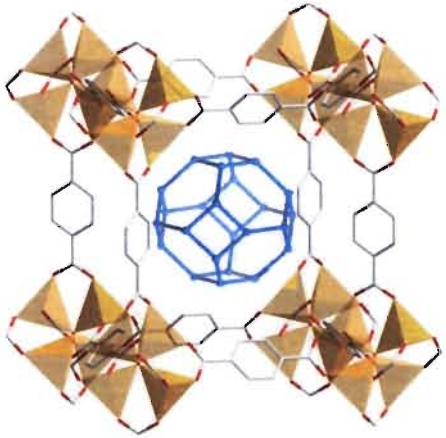

Porous Cage/Channel Structures

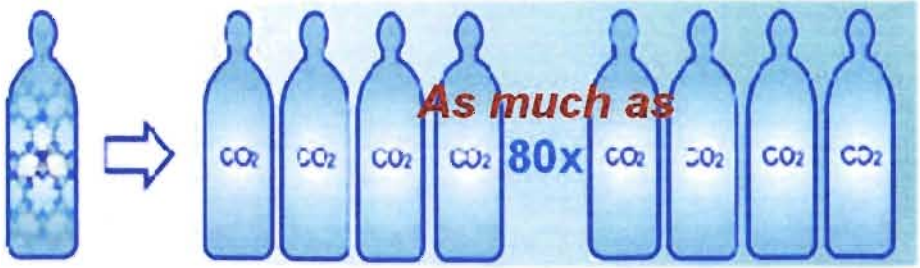

Molecular Encapsulation Frameworks

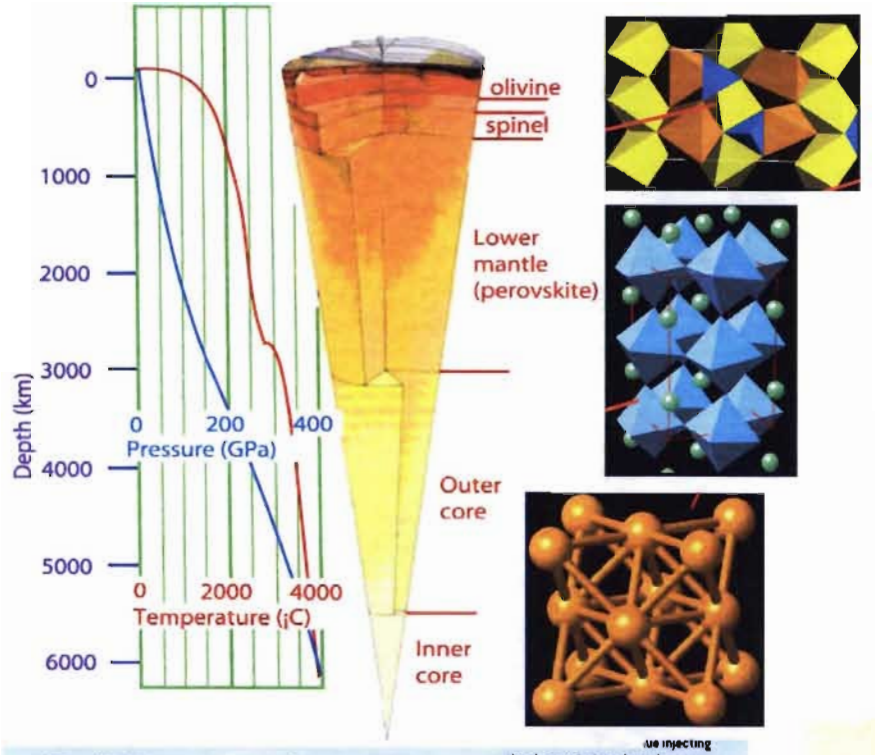

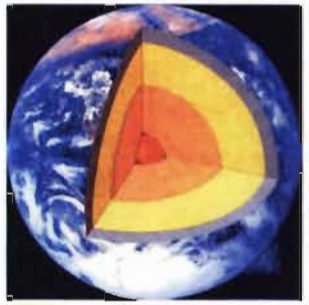

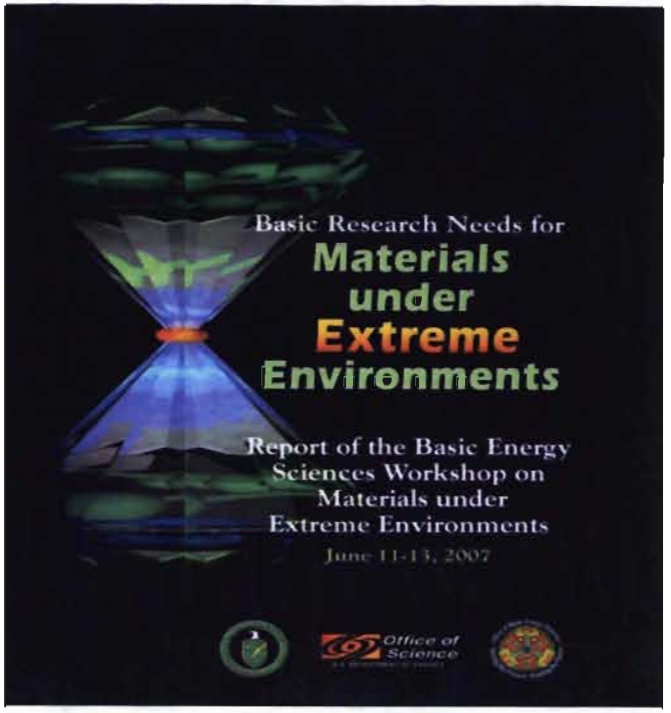

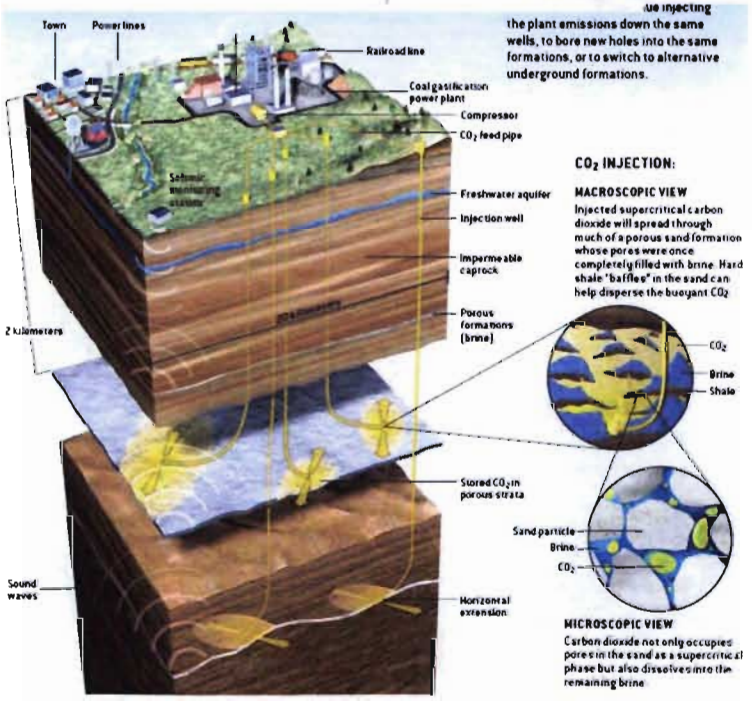

Perturbations to The System *far away from its equilibriums*

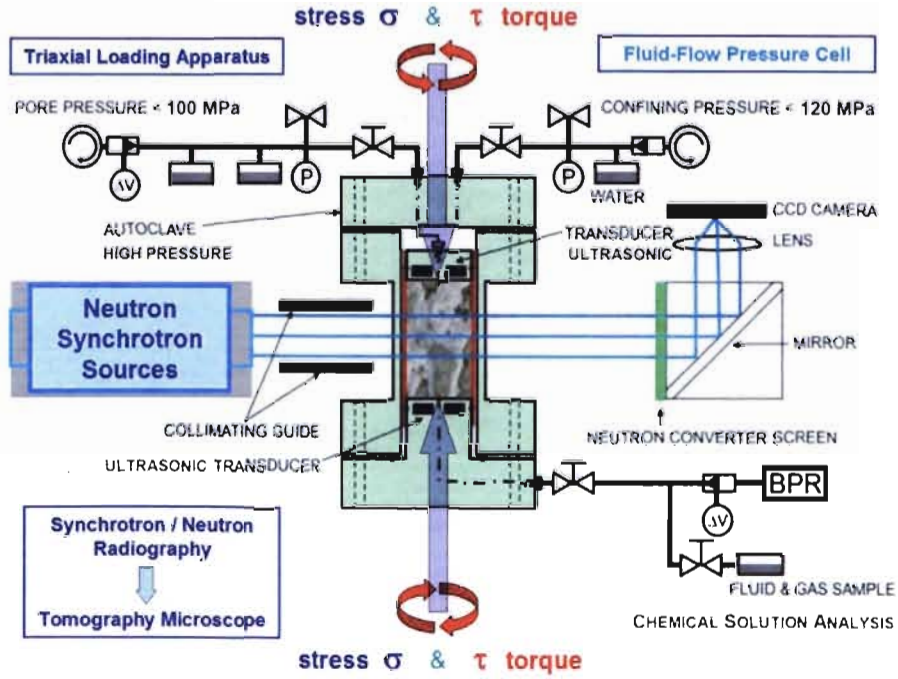

Hydrate stable

$P > P_d$

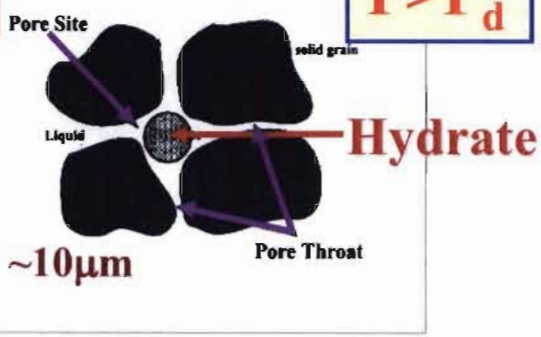

Gas Phase Patterns:

Effect of Pore-Size Distribution

$P < P_d$

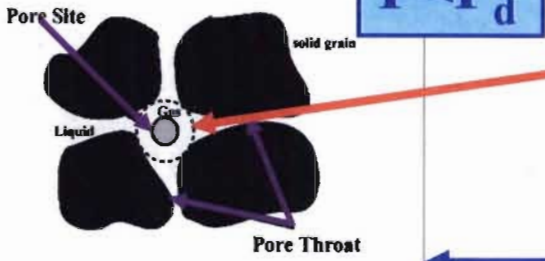

Hydrate dissociates

Pore-Network Schematics
Traps for gas and water

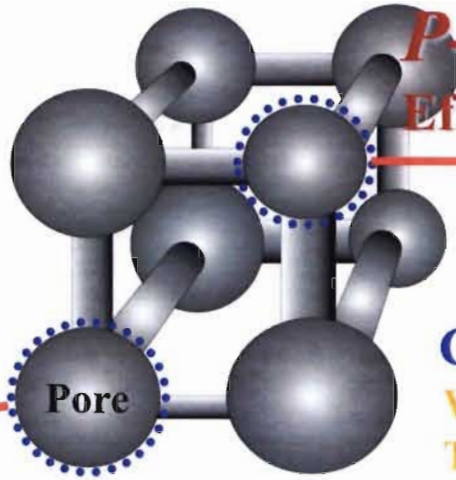

P-T Effects!

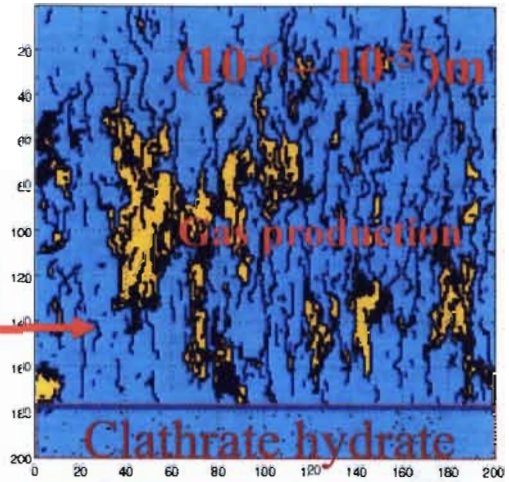

CH4

Water Trapped

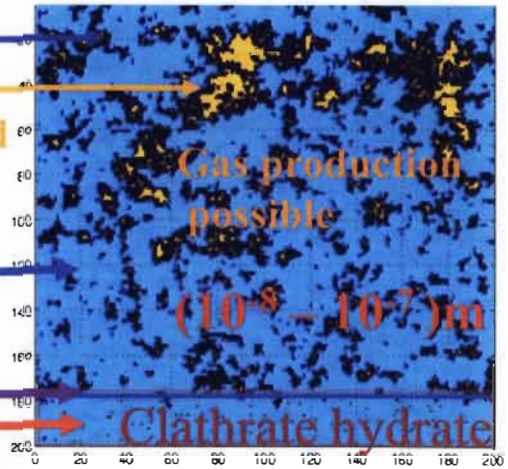

Hydrate Dissociation in a Single Pore

$P < P_d$

$P = P_d$

$P > P_d$

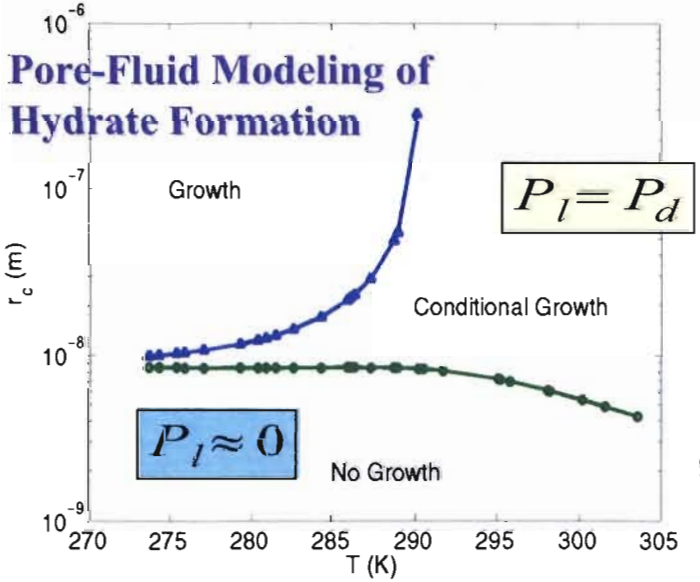

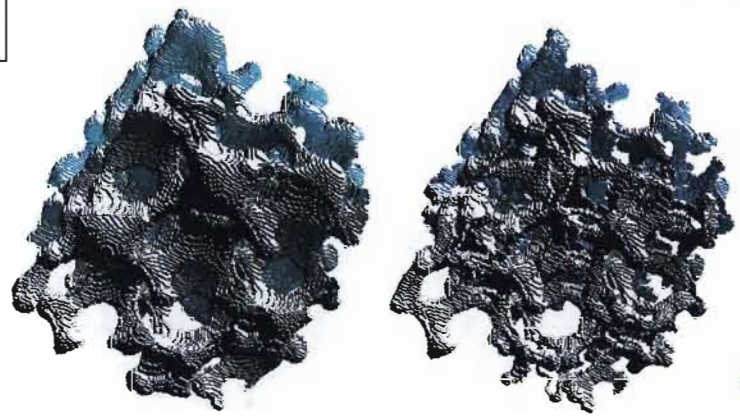

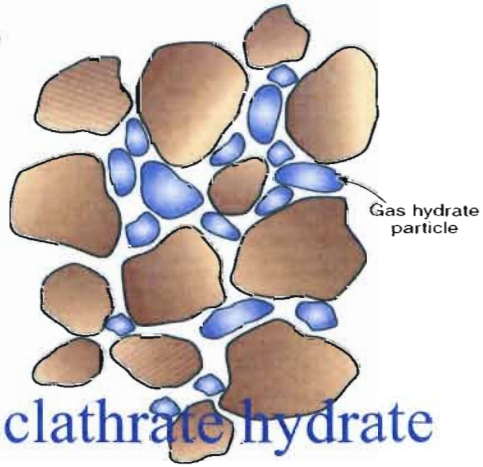

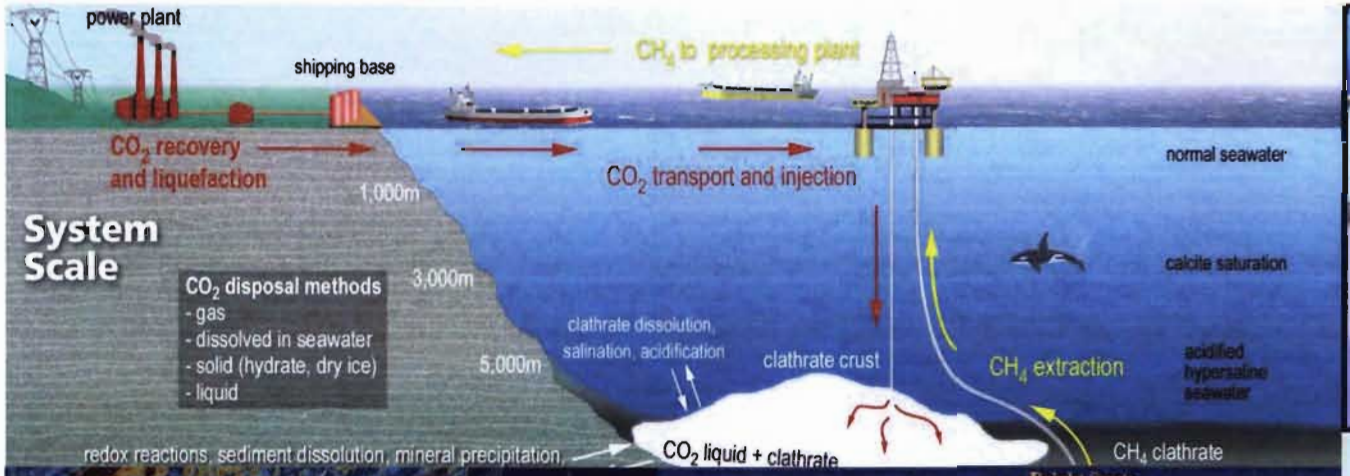

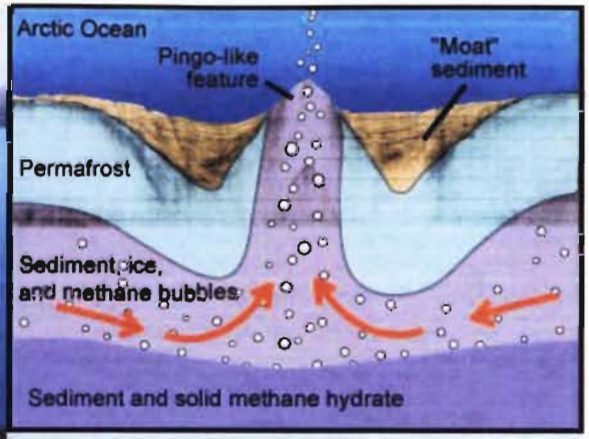

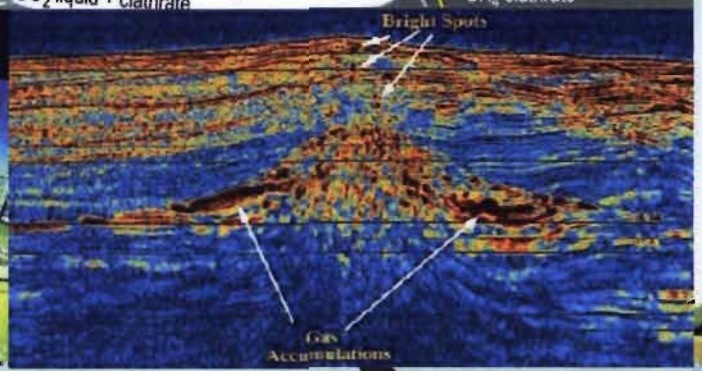

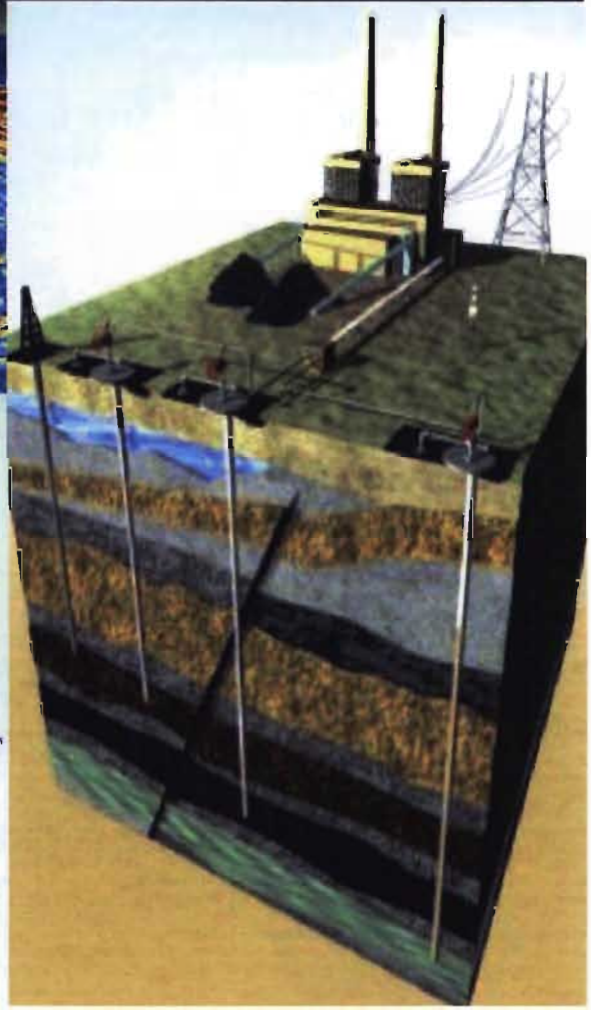

[Changes in porosity]

Pore Scale (10nm-10cm)

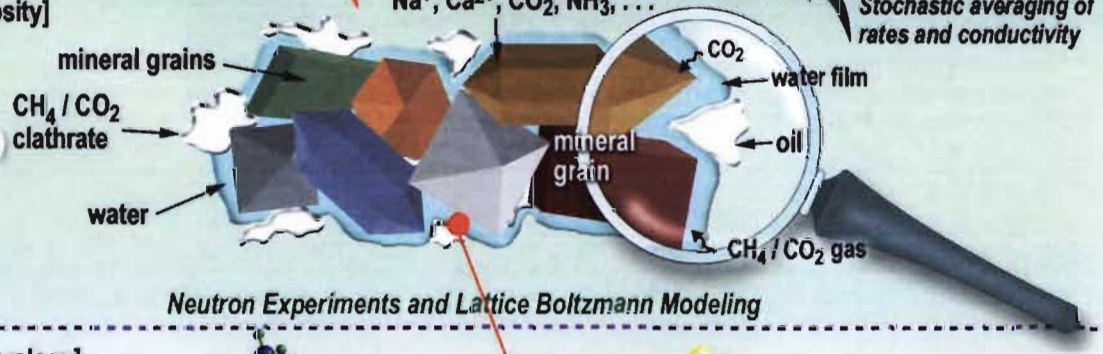

Stochastic averaging of rates and conductivity

Neutron Experiments and Lattice Boltzmann Modeling

[Changes in mineralogy]

Nanoscale (Å-10nm)

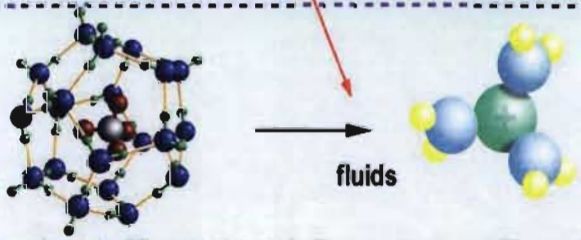

Mineral Fluid Experiments, Thermodynamic Parameters, and Theoretical Geochemistry

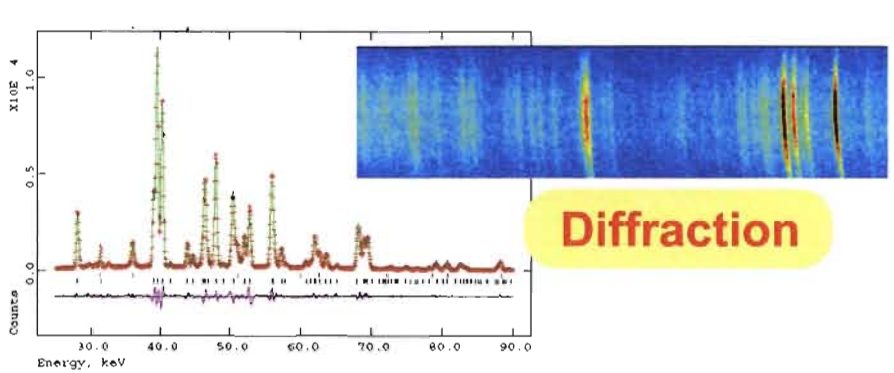

Diffraction

Tomography (*Strain*)

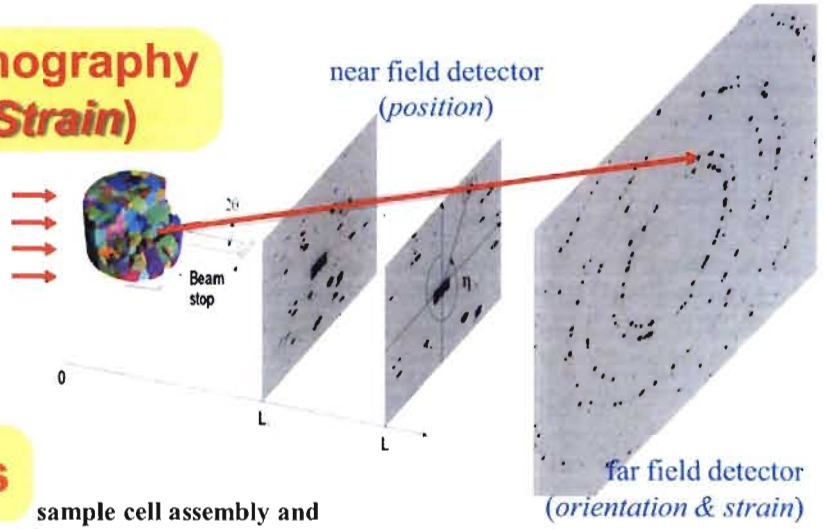

CCD/SSD

SSD/CCD detector

fluorescent screen (YAG crystal) and reflection mirror

Press

sample cell assembly and cubic anvil press (DIA)

CCD camera

Video camera

2nd mirror

Long working distance microscope (10X)

Incident slits

double crystal monochromator

upstream beam aperture

Motor driven incident slits (define incident beam size)

NSLS

Synchrotron x-ray

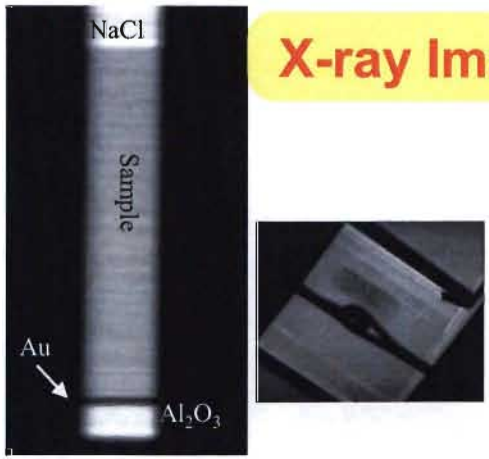

X-ray Imaging

Ultrasonic Interferometer

Simultaneous *P-V-T* EOS

Sound Velocity V_p, V_s &

Strain ε Tomography

Integrated Measurements

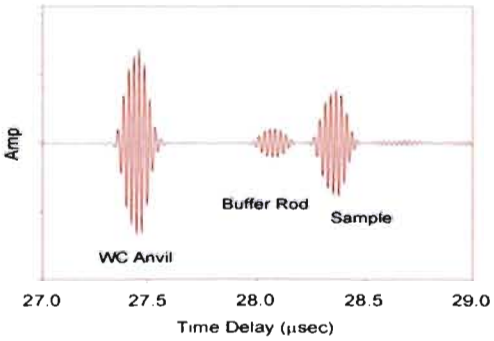

general & popular

Top Line & High End

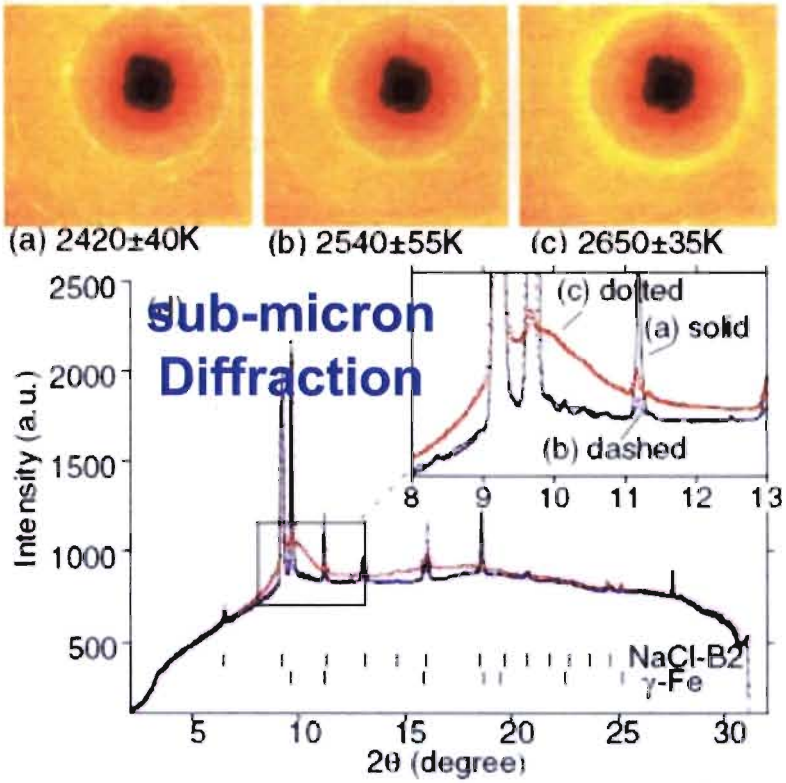

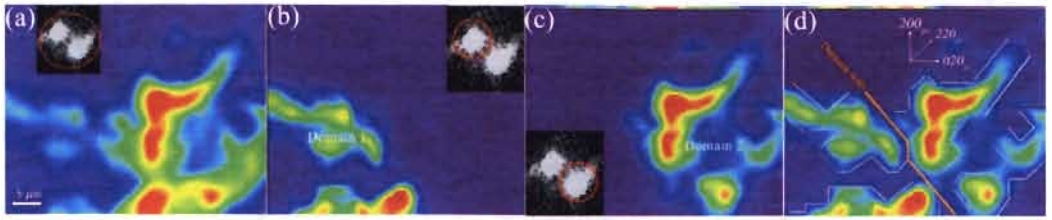

nano-imaging of domain wall in single crystal

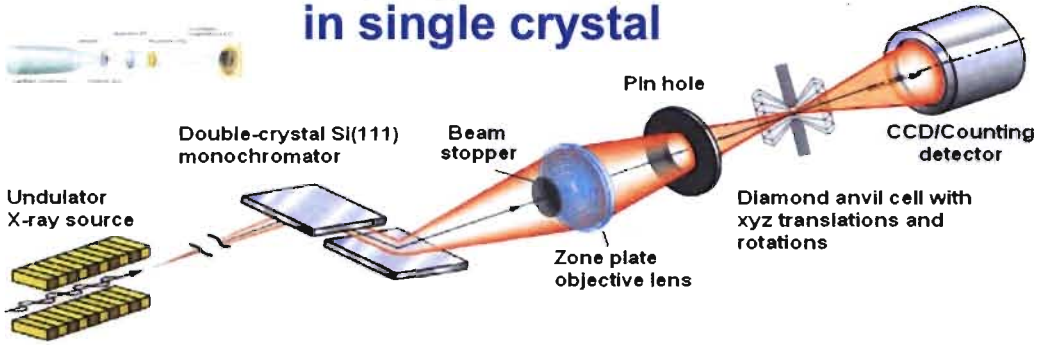

DAC Synchrotron Techniques

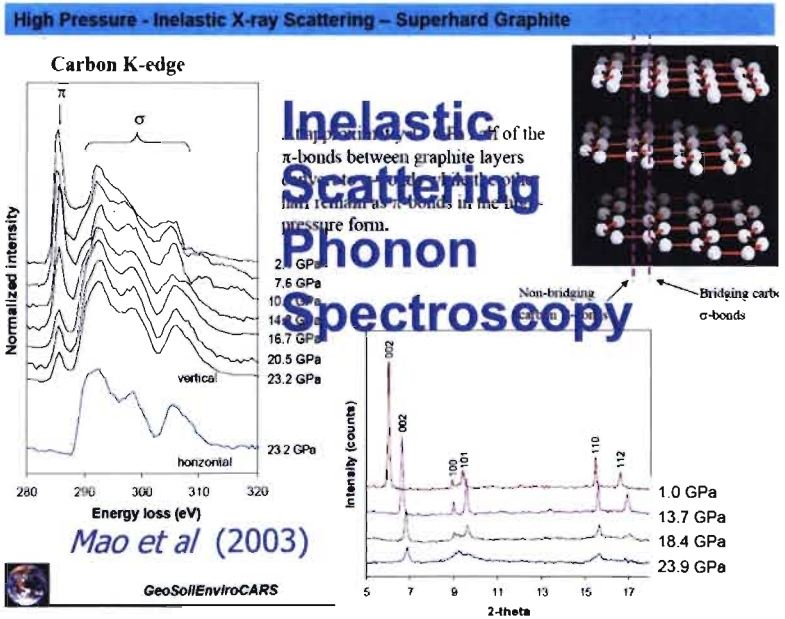

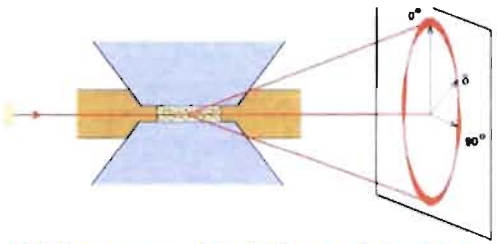

Stress & Elasticity

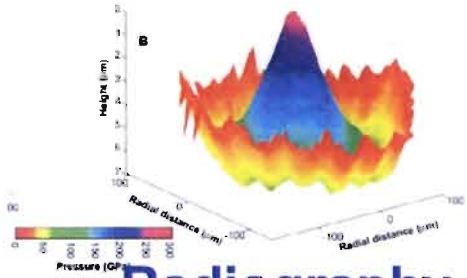

Radiography Tomography

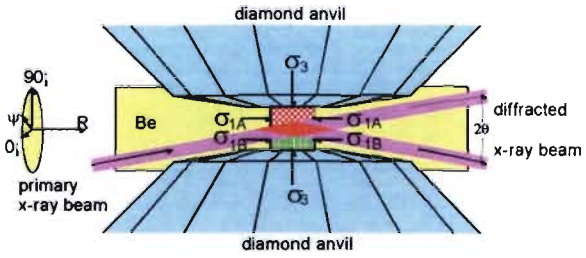

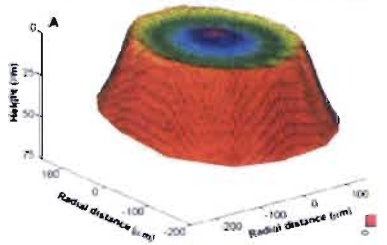

Schematic of the TXM setup at APS 32ID-C, SSRL 6-2

Nano-imaging

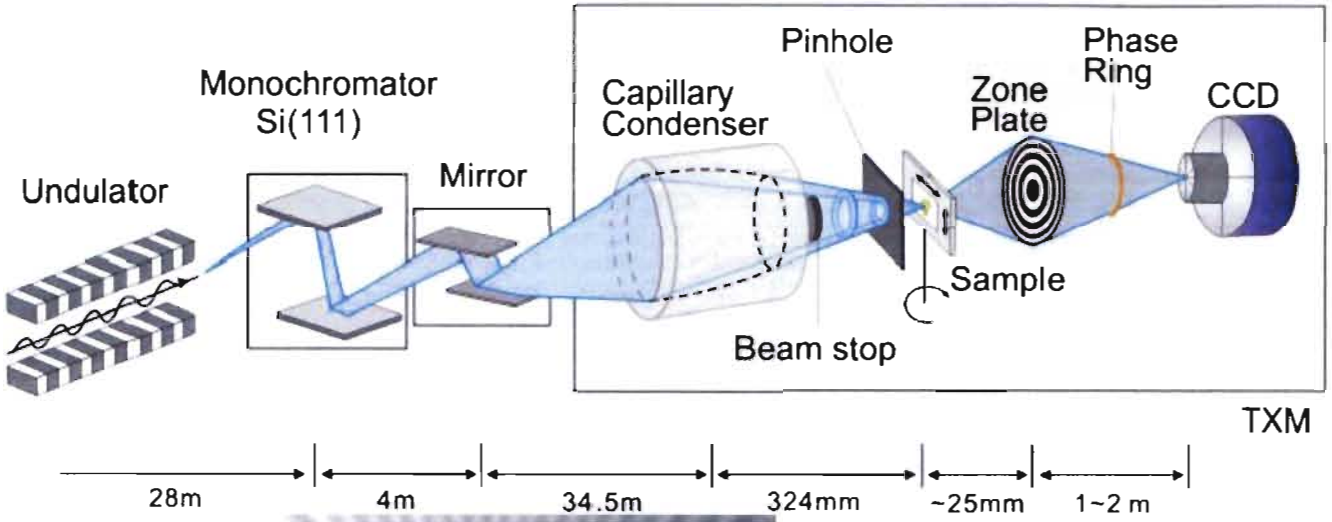

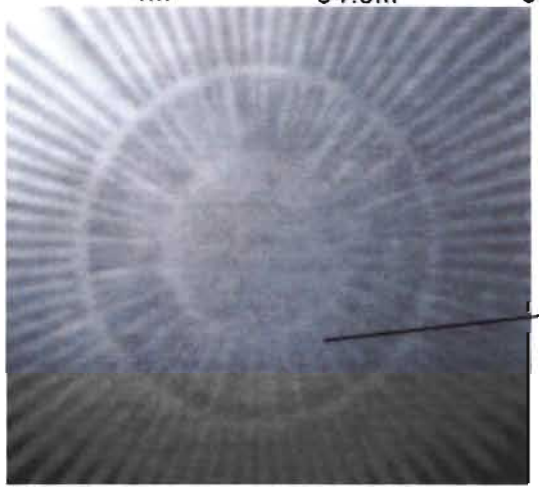

30 nm feature

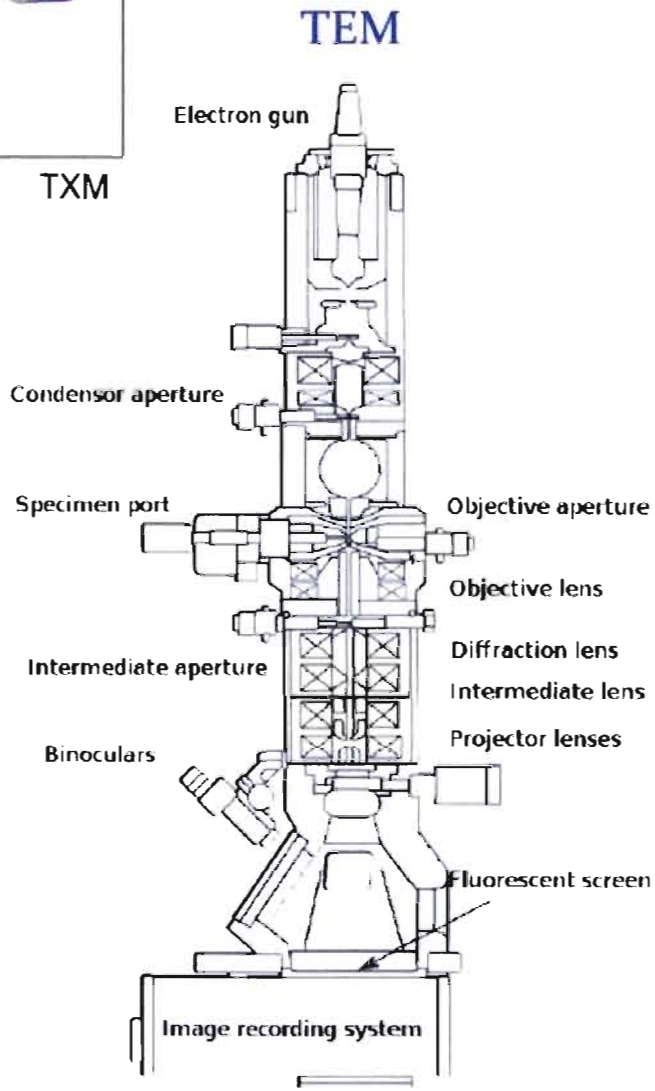

Beamline capabilities:

Full field imaging with 180 degrees data collection; 3d reconstruction with FOV 25 microns and 30 nm require uniform illumination for FOV (diffuser sometimes is used to create incoherent uniform beam)

Phonon Dynamics

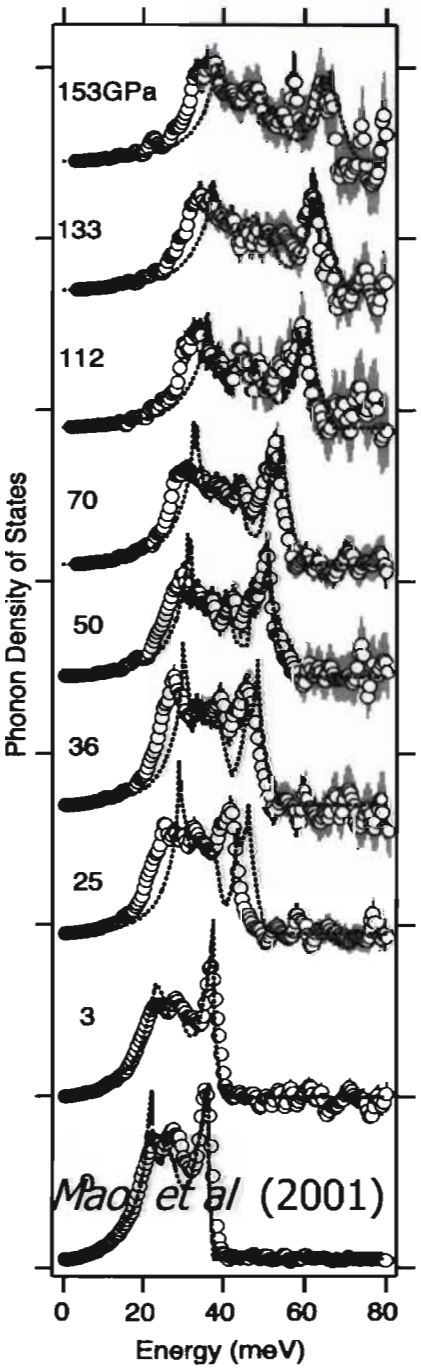

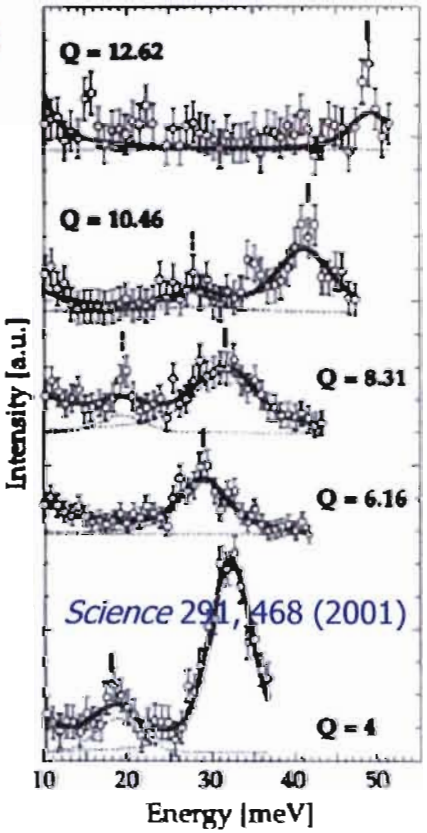

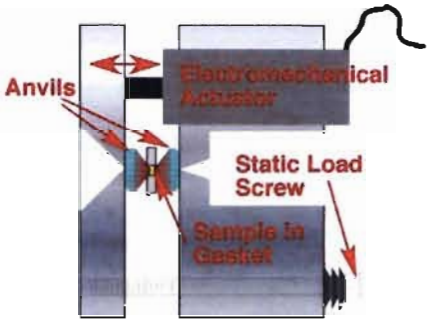

Dynamic DAC

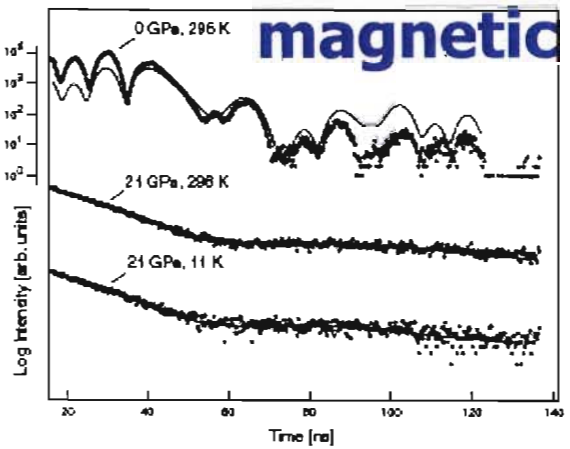

DAC Synchrotron Techniques

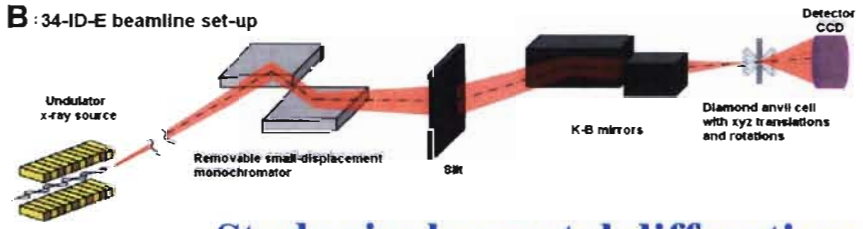

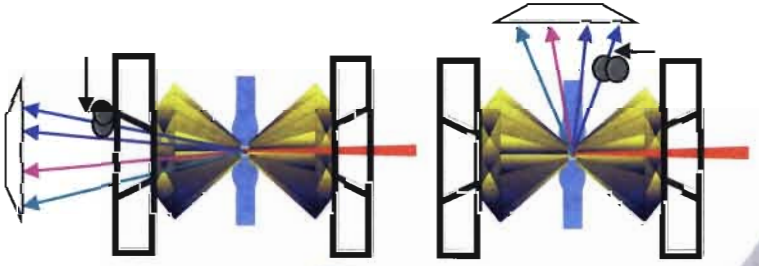

Laue - single crystal

Study single crystal diffraction in powder sample at high-P

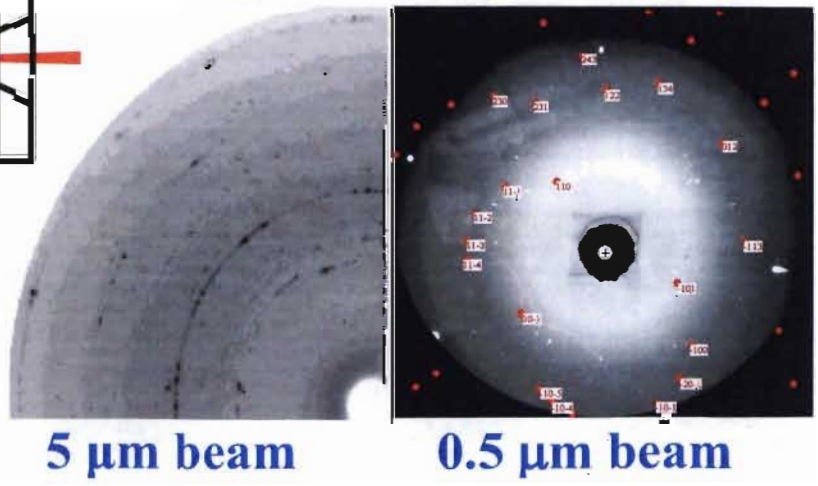

5 μm beam

0.5 μm beam

EFree Cold melting and solid structures of dense lithium

Christophe L. Guillaume, Eugene Gregoryanz, Olga Degtyareva, Malcolm I. McMahon, Shaun Evans, Michael Hanfland, Malcolm Guthrie, Stas V. Sinogeikin, & H-K. Mao, *Nature Physics* **7**, 211 (2011)

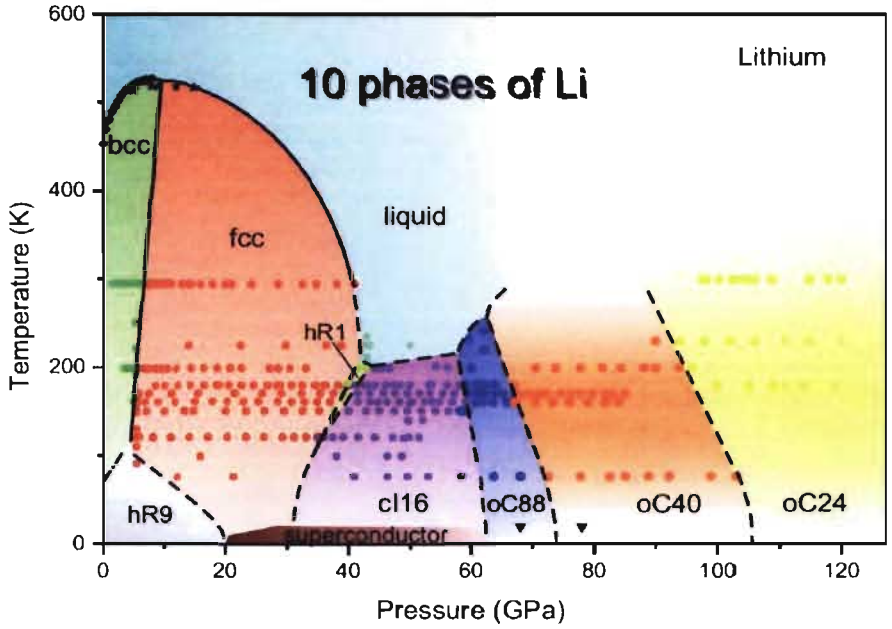

β-tin → Imma → sh phases & superconductivity of Ge

Xiao-Jia Chen 陈晓嘉, Chao Zhang, Yue Meng, Rui-Qin Zhang, Hai-Qing Lin, Viktor V. Struzhkin, and Ho-kwang Mao, *Phys. Rev. Lett.* ***106***, 135502 (2011)

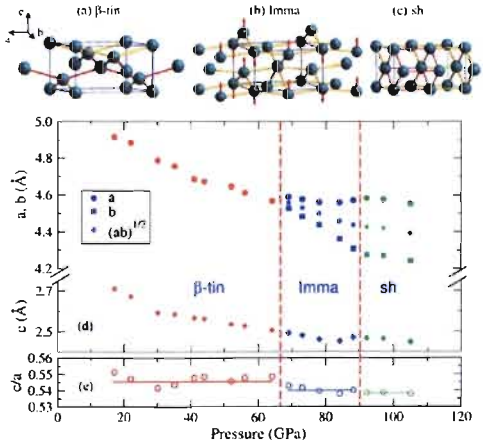

10 phases of Ge

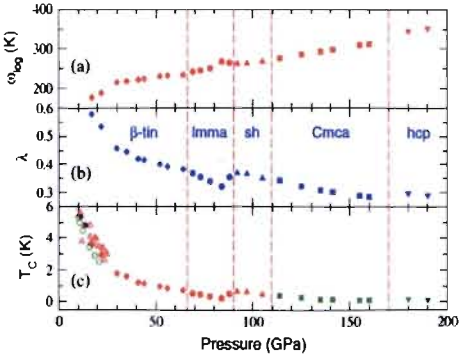

Change of Free Electron Metal to Insulation

Can we follow the process through their plasmons?

Na phase diagram, Gregoryanz et al, *PRL* (2005); *Science* (2008)

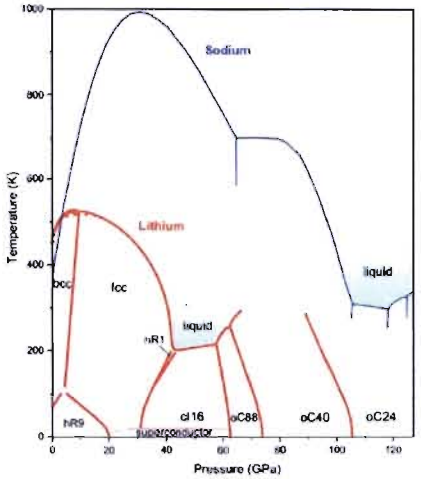

Transparent Na, Ma et al, Nature (2009)

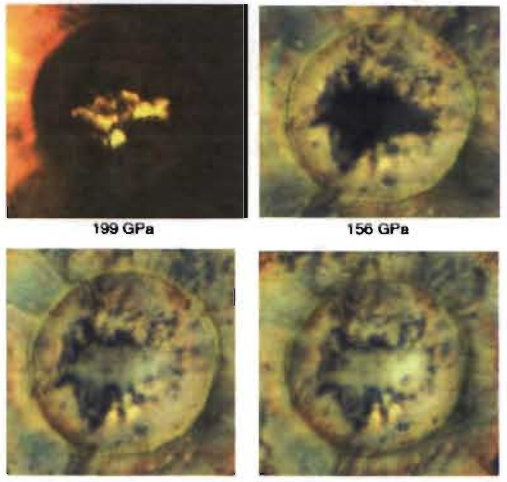

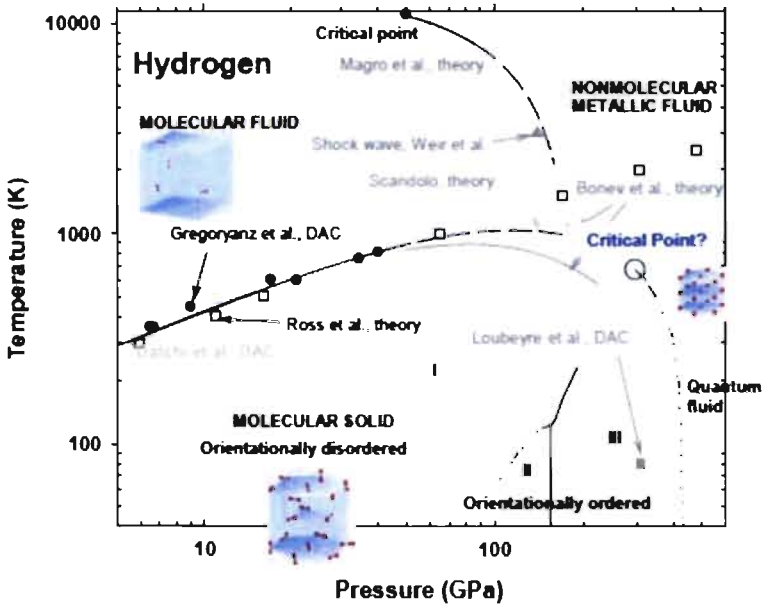

Metallic Hydrogen – A 75-year long prediction of exotic phenomena

- A room Tc superconductor?
- A zero-T metallic superflud?
- electron and proton quantum fluids?

Needs >450 GPa and *in-situ* probes

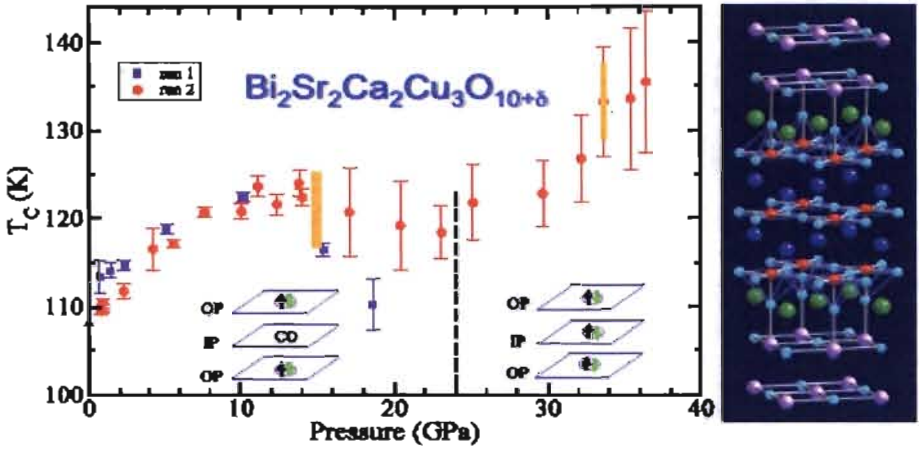

Chen et al, *Nature* ***466***, 950 (2010),Enhancement of superconductivity by pressure-driven competition of ordering

Baldini. et al, *PRL* ***106***, 066402 (2011), LaMnO3 is not a standard Mott insulator at pressure-induced metallization.

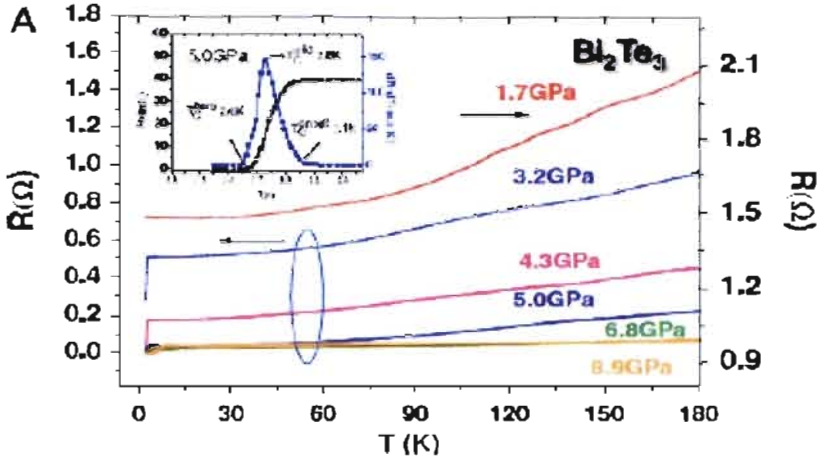

Zhang,JL. et al, *PNAS* ***108***, 24 (2011)

First observation of a pressure-induced superconductivity in Bi_2Te_3 which keeps its unique topological insulating characteristics

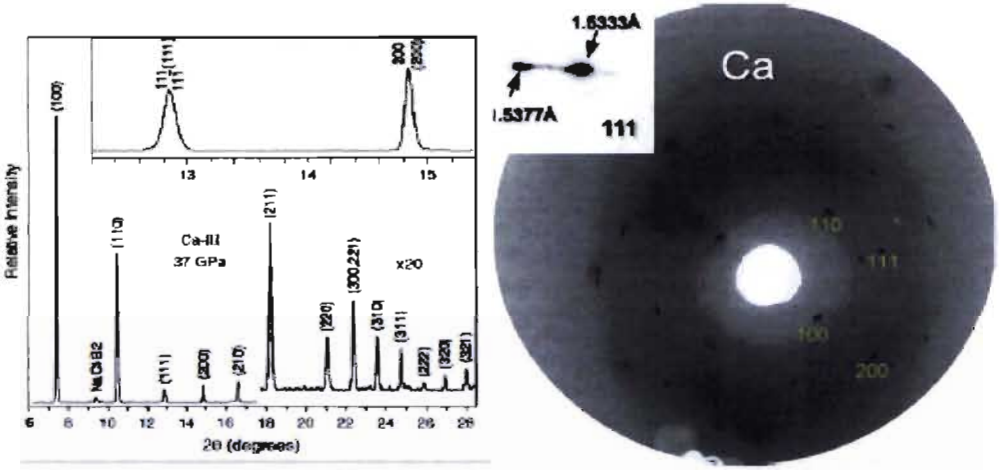

Mao, W. et al, *PNAS* ***107***, 9965 (2010)

Crystal structure of calcium which turns into the record high Tc (26 K) superconductor among all elements 8 HP phases

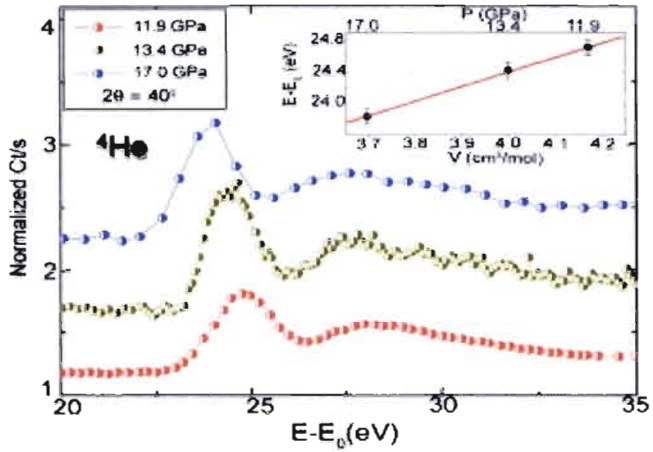

Mao, H. et al, *PRL* ***105***, 186404 (2010)

High-pressure excitonic and electronic dynamics of crystalline ^{4}He which has the highest energy bandgap of all known materials.

Pressure tuning and transforming superconductors, topological insulator, wide-gape insulator, metal,and spintronic materials

Shanghai Synchrotron Radiation Facility (SSRF)

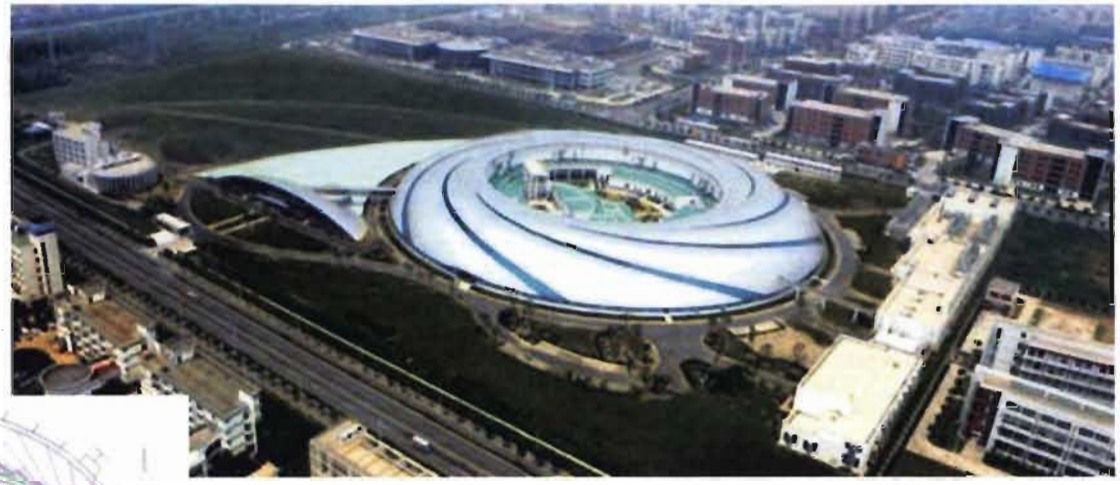

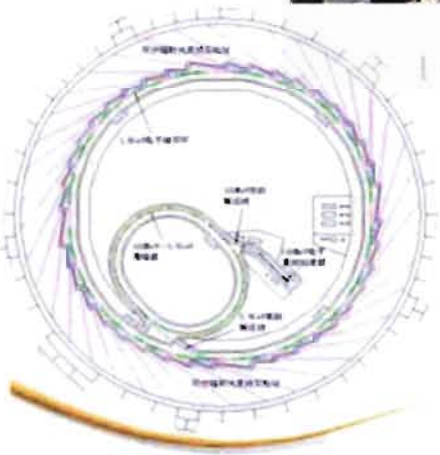

Spatial Resolution:

sub –μm

Energy Resolution:

m eV

Time Resolution:

sec.

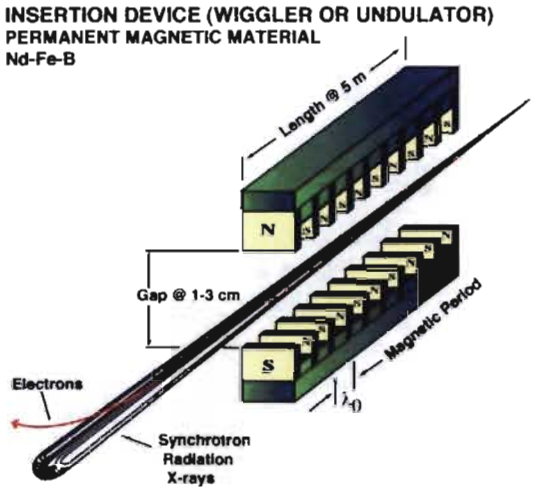

Dedication to High-*P* Works:

we recommend to build a undulator beamline for DAC and a super-conducting wiggler beamline for LVP.

Philosophy!

A high-end "Farrari" and a well-functional "Volkswagen"

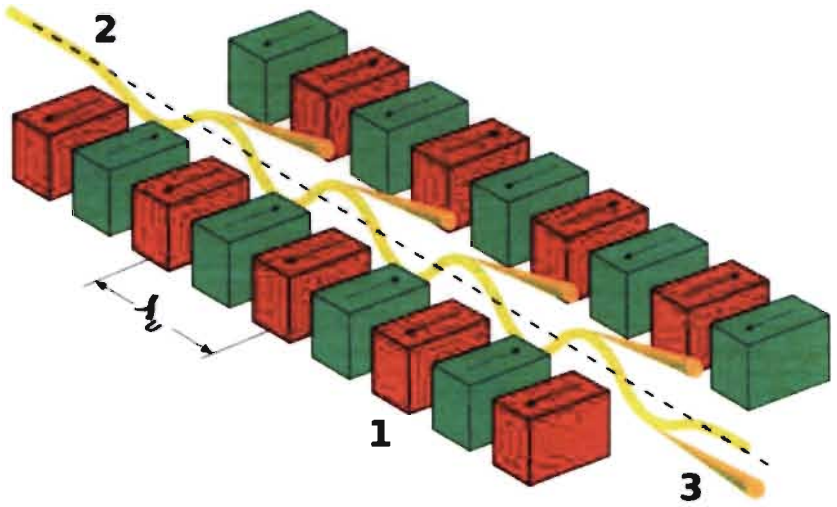

DAC

diffraction / spectroscopy:

10-30 keV

mono. → brilliance!

→ Undulator

DAC : Brilliance hungry (*typical size: 10 μm*)

LVP : Flux hungry (*typical sample: 1 mm*)

LVP

diffraction / imaging:

20-100 keV

mono & white → flux!

→ S.C. Wiggler

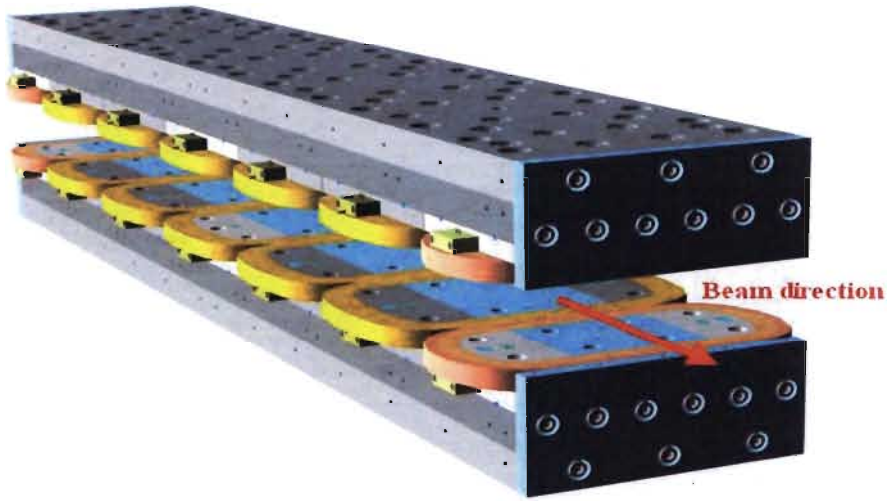

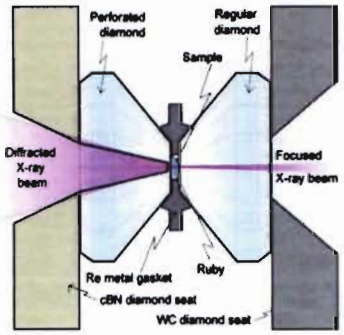

HPSynC

the way to go!

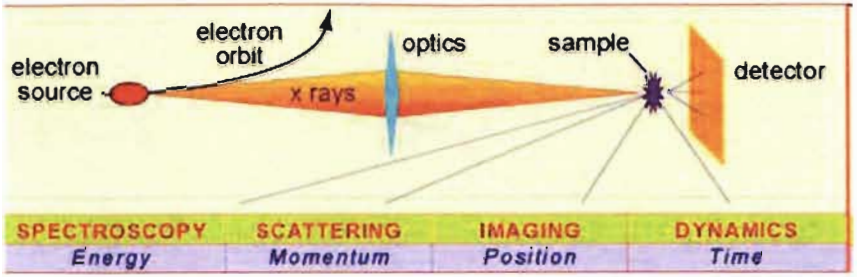

Nuclear resonant inelastic scattering;

Resonant x-ray emission spectroscopy;

X-ray emission spectroscopy;

Nuclear forward scattering;

Energy /Angle dispersive;

White beam Laue;

Single crystal diffraction;

Inelastic x-ray scattering (x-ray Raman);

X-ray absorption fine structure spectroscopy

High resolution micro-diffraction/tomography;

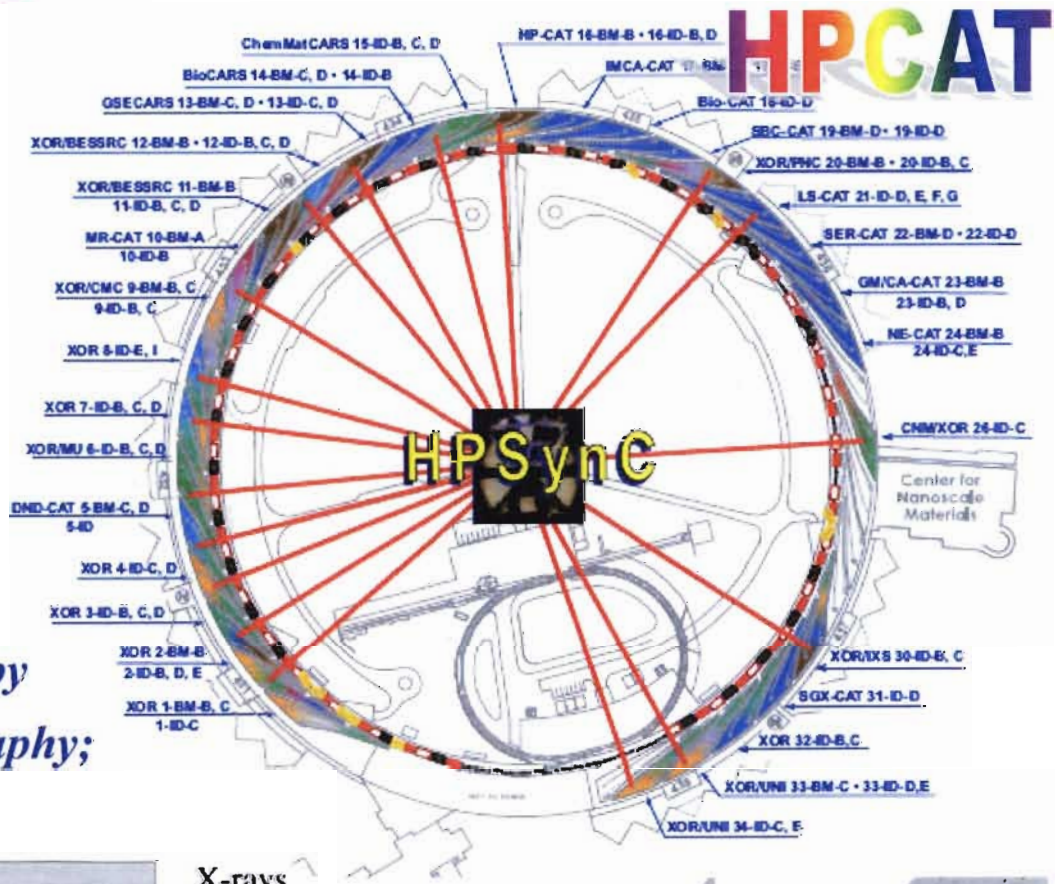

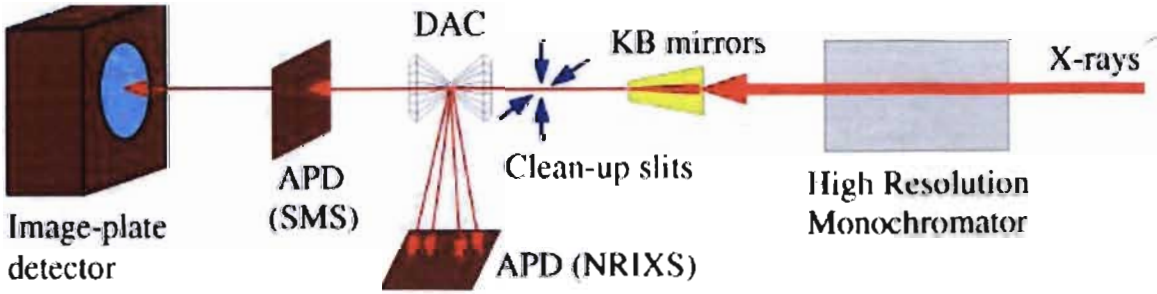

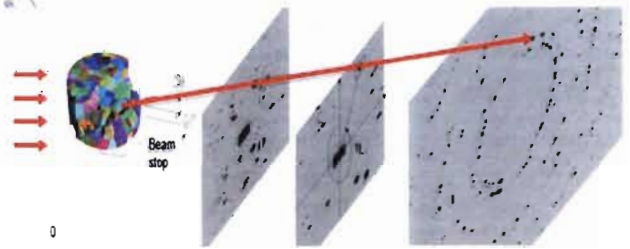

Mission: high risk, high return, high pressure synchrotron radiation science and technique developments by combining the extreme conditions(P,T,H) with SR spectroscopy, scattering, imaging and dynamics studies

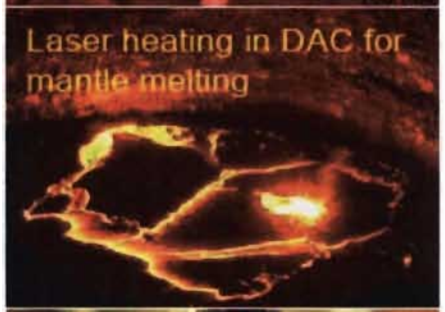

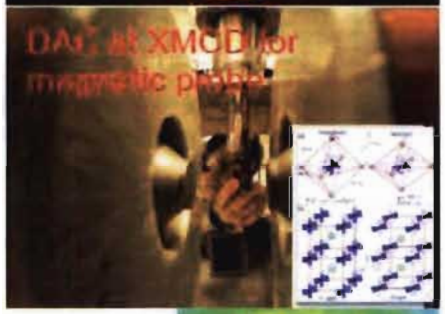

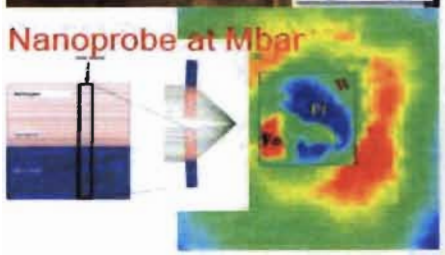

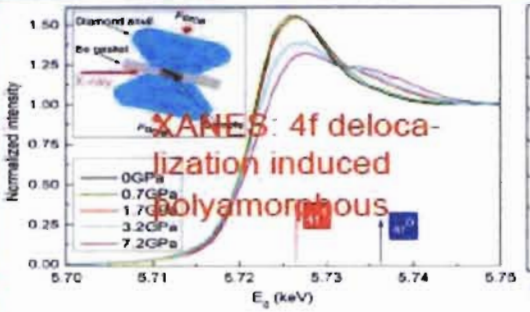

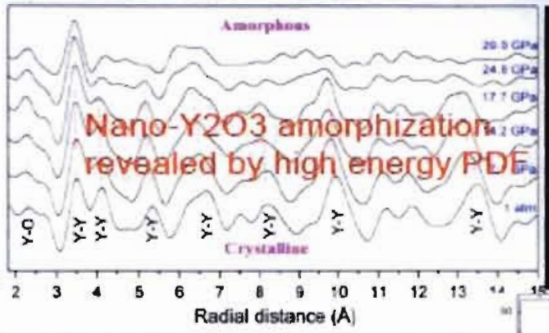

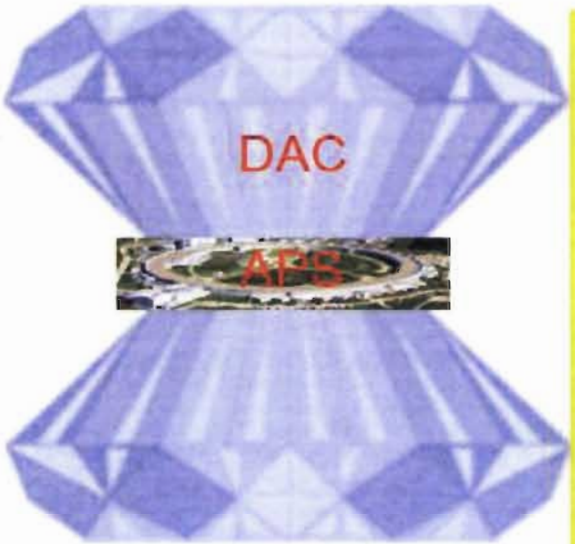

Advantage of SR:
High brilliance
Tunable
High spatial res.
High energy
High energy res.
Coherent
Polarization
Time resolved